Elsevier Editorial System(tm) for Chemical Engineering Journal

Manuscript Draft

Manuscript Number: CEJ-D-19-06587

Title: Experiments of methylene blue and lead (II) adsorption onto raw and modified PEI silica from Bouillante geothermal fluids (Guadeloupe, FWI) for possible treatments of contaminated natural waters.

Article Type: Research Paper

Section/Category: Environmental Chemical Engineering

Keywords: geothermal silica, methylene blue, lead, adsorption, kinetic model, isotherm model

Corresponding Author: Mrs. Christelle Dixit,

Corresponding Author's Institution: Université des Antilles

First Author: Christelle Dixit

Order of Authors: Christelle Dixit; Chaker M Ncibi; Sarra Gaspard; Marie-Lise Bernard; Bernard Sanjuan

Abstract: This study aims to evaluate the possibility of using silica extracted from Bouillante geothermal waters (Guadeloupe, FWI) as an adsorbent for the remediation of natural waters. The raw silica SiO2 was tested as well as a modified silica called PEI/SiO2 and prepared by grafting polyethyleneimine (PEI) onto raw silica surfaces. The presence of the PEI molecules onto SiO2 surface was confirmed by X-ray photon spectroscopy (XPS) and Fourier transform infrared (FTIR) analysis. The changes in their porous structures were evaluated by N2 adsorption at 77K.
The adsorption capacities of SiO2 and PEI/SiO2 were investigated for two contaminants: methylene blue (MB) and lead (Pb). The influence of various parameters (pH, temperature, initial concentration, adsorbent dosage) was studied. Adsorption isotherms were fitted with the Langmuir, Freundlich and Redlich-Peterson and Brouers-Sotolongo models and the kinetic data with pseudo-first-order and pseudo-second-order models.
The results show that raw SiO2 has an interesting adsorption capacity towards methylene blue (qe = 108 mg.g-1), with no significant enhancement of the adsorption capacity with the PEI grafted silica. On the other hand, the PEI grafting significantly improved the adsorption capacity of geothermal silica for lead (qe increases from 5.3 mg.g-1 to 18 mg.g-1). For both pollutants, the data modeling reveals that the adsorption kinetics corresponds well with pseudo-second order kinetic model suggesting a chemisorption, and the adsorption isotherms are in agreement with Redlich-Peterson model.

Suggested Reviewers: Oscar G. M. Sandoval
Faculty of Chemical Sciences and Engineering, Baja California Autonomous University
gmiranda@uabc.edu.mx

He published a paper on the use of Amorphous silica waste from a geothermal central as an adsorption agent of heavy metal ions for the regeneration of industrial pre-treated wastewater.

Laurence Bois
Laboratoire Multimatériaux et Interfaces, Université Claude Bernard
laurence.bois@univ-lyon1.fr
She worked on the use of mesoporous silica, its characteristics and its adsorption properties.

Özgül Gerçel
Department of Environmental Engineering, Anadolu University
ogercel@anadolu.edu.tr
He is an expert in the adsorption process of pollutants by a wide variety of adsorbents.

Opposed Reviewers:

Supplementary Information

Experiments of methylene blue and lead (II) adsorption onto raw and modified PEI silica from Bouillante geothermal fluids (Guadeloupe, FWI) for possible treatments of contaminated natural waters.

Christelle Dixit, Chaker Mohamed Ncibi, Sarra Gaspard, Marie-Lise Bernard, Bernard Sanjuan

Geothermal silica

This is a picture of geothermal silica taken on the surface installations of the Bouillante geothermal power plant (French West Indies). It illustrates the key element of our work: an industrial waste that we want to promote as a byproduct of electricity production.

List of Suggested Reviewers

Name	Institution	E-mail Address
Oscar G. M. **Sandoval**	Baja California Autonomous University	gmiranda@uabc.edu.mx
Laurence **Bois**	Université Claude Bernard	laurence.bois@univ-lyon1.fr
Özgül **Gerçel**	Anadolu University	ogercel@anadolu.edu.tr

Highlights

- Geothermal silica can be used as absorbent to treat contaminating natural waters
- Unmodified geothermal silica effectively removes methylene blue
- Amino groups improve silica efficiency for the removal of heavy metals such as lead

Experiments of methylene blue and lead (II) adsorption onto raw and modified PEI silica from Bouillante geothermal fluids (Guadeloupe, FWI) for possible treatments of contaminated natural waters.

Christelle Dixit[a,*], Chaker Mohamed Ncibi[b1], Sarra Gaspard[b], Marie-Lise Bernard[a], Bernard Sanjuan[c]

[a] LaRGE, EA 4935, Campus de Fouillole, Université des Antilles, 97159 Pointe-à-Pitre, Guadeloupe, France

[b] COVACHIM-M2E, EA 3592, Campus de Fouillole, Université des Antilles, 97159 Pointe-à-Pitre, Guadeloupe, France

[c] BRGM, 3 Av. Claude Guillemin, BP6009, 45060 Orléans Cedex 02, France.

*Corresponding author. E-mail address: christelle.dixit@univ-antilles.fr

Abstract

This study aims to evaluate the possibility of using silica extracted from Bouillante geothermal waters (Guadeloupe, FWI) as an adsorbent for the remediation of natural waters. The raw silica SiO_2 was tested as well as a modified silica called PEI/SiO_2 and prepared by grafting polyethyleneimine (PEI) onto raw silica surfaces. The presence of the PEI molecules onto SiO_2surface was confirmed by X-ray photon spectroscopy (XPS) and Fourier transform infrared (FTIR) analysis. The changes in their porous structures were evaluated by N_2 adsorption at 77K. The adsorption capacities of SiO_2 and PEI/SiO_2 were investigated for two contaminants: methylene blue (MB) and lead (Pb). The influence of various parameters (pH, temperature, initial concentration, adsorbent dosage) was studied. Adsorption isotherms were fitted with the Langmuir, Freundlich and Redlich-Peterson and Brouers-Sotolongo models and the kinetic data with pseudo-first-order and pseudo-second-order models.

[1] C. M. Ncibi Department of Green Chemistry, School of Engineering Science, Lappeenranta University of Technology, Sammonkatu 12, FI-50130 Mikkeli, Finland.

The results show that raw SiO_2 has an interesting adsorption capacity towards methylene blue (q_e = 108 $mg.g^{-1}$), with no significant enhancement of the adsorption capacity with the PEI grafted silica. On the other hand, the PEI grafting significantly improved the adsorption capacity of geothermal silica for lead (q_e increases from 5.3 $mg.g^{-1}$ to 18 $mg.g^{-1}$). For both pollutants, the data modeling reveals that the adsorption kinetics corresponds well with pseudo-second order kinetic model suggesting a chemisorption, and the adsorption isotherms are in agreement with Redlich-Peterson model.

Keywords: geothermal silica, methylene blue, lead, adsorption, kinetic model, isotherm model

1. Introduction

In numerous regions in the world, the pollution of natural waters is a real environmental problem, since the soil and groundwater are contaminated by very persistent pollutants. As an example, in Guadeloupe (French West Indies) chlordecone and beta-HCH are presently very problematic agricultural pollutants [1]. The preferential treatment currently used for the treatment of polluted water is adsorption on activated carbon. The use of activated carbon - which is a carbon-based material with a very porous structure - is considered to be one of the best procedures of removing pollutants in solutions [2], but its development remains constrained by its high price [3]. A solution can be the development of activated carbon from local agricultural waste such as coconut shell, banana stem and trunks [4–6] or for vetiver roots [7].

Another alternative can be the development of new absorbent materials as effective as activated carbon and with lower costs. In this context, silica extraction from geothermal waters and its use in the production of new adsorbents for the treatment of contaminated natural waters could have an economic interest. Few studies have been leaded on the use of unmodified and modified geothermal silica as a commercial absorbent [8,9]. In this context, it seems to us interesting to study the adsorption capacity of geothermal silica from Bouillante geothermal power plant, in order to evaluate the possibility of using this industrial waste as a byproduct of energy production.

The Bouillante geothermal field, located on the west coast of Basse-Terre in Guadeloupe, is a high temperature field (250 - 260°C), that allows electricity production. The power station has presently a total capacity of about 15 MWe, which represents a total fluid discharge of 600 tons h^{-1} and 120 tons.h^{-1} of steam, after phase separation. The high-temperature fluid discharged from the geothermal reservoir through the wells contains various dissolved species such as silica and metal ions which can precipitate during the fluid exploitation (especially during their cooling) to form troublesome scale deposits like amorphous silica or poly-metallic sulfides [10,11]. Deposits of hard adherent silica are regularly observed on low-temperature surface installations at Bouillante and

bring the production to recurring standstills in order to remove them. The abundance of these deposits and the difficulty to remove them represent additional expenditure for the operator. These scales can also precipitate in the wellbore during reinjection of geothermal waste-water and quickly decrease the injectivity and the permeability of the wells.

A solution to prevent silica precipitation consists in removing the excess of dissolved silica, with formation of colloidal particles, before the re-injection. The main developed methods are based on the controlled precipitation by addition of silica gel and other precipitants such as metal salts [12,13], the use of fluidized-bed reactor [14] or the simple ultrafiltration after silica polymerization. There is a twofold advantage of silica removal as it allows 1) the mitigation of the problems associated with the precipitation of amorphous silica by reducing the concentration of silica in geothermal water and 2) the commercial valorization of silica as a byproduct. The initial silica concentration is about 500 $mg.L^{-1}$ at Bouillante [10,15]. So, from 600 tons of water produced per hour, more than 7 tons of silica could be extracted each day if we consider precipitation of all dissolved silica. This geothermal silica, considered as an industrial waste, is characterized by a high purity (98 %) and a high specific surface area (~ 200-300 $m^2.g^{-1}$), properties close to those of commercial silica [15]. In view of these characteristics, this geothermal silica could be an effective and low cost alternative to carbon material for waste water treatment.

In this paper, we present a study on the adsorption of methylene blue (MB) and lead (II) onto unmodified geothermal silica gel (SiO_2) and onto geothermal silica modified with a cationic surfactant, the polyethylenimine (PEI/SiO_2), in order to enhance its adsorption capacity toward organic compounds. Indeed, most reported works [16–19] show that heavy metals are more efficiently adsorbed on mesostructured silica modified with organic chains containing one or more amino groups. The adsorption kinetic and isotherm were investigated using batch experiments, under different pH and temperature conditions. Silica was characterized, before and after PEI adsorption, by various physico-chemical techniques such as Fourier transform infrared, X-ray photon spectroscopy, electronic microscopy and Nitrogen absorption method, in order to confirm

that PEI had been grafted onto the surface of silica particles and to have insights on the adsorption mechanisms.

2. Materials and methods

2.1. Preparation and characterization of PEI/SiO_2 composite

Generally, silica gel (natural or synthetized) is an ideal support which possesses high surface area and good adsorption properties [20–23]. On the other hand, silica is strongly hydrophilic and doesn't have good adsorption capacities to remove organic molecules in aqueous solution. Moreover, mineral oxide surfaces as silica can be modified by surfactant coating in order to enhance their adsorption capacity toward organic compounds. This change allows combining the specific chemical properties of an organic molecule to the physical properties of the silicic matrix in order to obtain organic-inorganic hybrid materials for specific applications. Among organic molecules which can be used for the functionalization of silica, those with amino groups - seem to be the most effective for the removal of heavy metals such as cadmium, zinc, copper, chromium or lead [16–19,24–26]. The polyethyleneimine (PEI) is a water-soluble synthetic polymer belonging to polyamine group. PEI chemical structure (Fig.1) shows a line-type macromolecular chains containing a large quantity of nitrogen atoms of amino groups, which can produce very strong chelating action for heavy-metal ions [27,28]. In dilute solution, the polyelectrolyte may form a film around the particles in solution allowing decreasing their surface tension. As a result, when the PEI is attached to another molecule, it is often assimilated to a cationic surfactant. Therefore, it can be used to stabilize hydrophobic colloidal suspensions such as colloidal silica.

The silica used to carry out this study comes from the water discharged from the Bouillante geothermal reservoir through deep wells, after phase separation. Previously, Dixit et al. [15] carried out an experimental study on the kinetics of silica precipitation during cooling of the Bouillante geothermal fluid. It was observed that dissolved silica precipitated only under colloidal form during the experiments and the colloids were mainly constituted of amorphous silica.

In this study, separated water was collected at 30°C in plastic jerrycan from a fixed fluid sampling point located after the HP separator phase. The samples were directly obtained at the relevant working temperature, using a suitable cooling system composed of a tank with a small submerged streamer. Upon cooling, the dissolved SiO_2 precipitated and polymerized to form colloidal suspension after few hours. This silica gel was extracted by filtration and dried to obtain the solid silica SiO_2, used thereafter. The polyethyleneimine (PEI) used in this study was a commercial solution from Aldrich company, composed of branched polymer at 50% (w/v) in H2O (M_w ~ 750,000) with 25%, 50% and 25% of I, II and III amino groups, respectively. Synthetic solutions from this surfactant were prepared by dissolving a given amount of concentrated PEI liquid in distilled water and subsequently diluting this solution to obtain the required concentrations. PEI concentrations were measured by spectrophotometry considering absorbance maxima. An UviLine 9400 spectrophotometer from SCHOTT Instruments was operated at the wave-length of 290 nm. The precision of the UV-visible spectrophotometer is typically about 0.3% (0.003 A).

The preparation of the modified geothermal silica samples, referred as PEI/SiO_2, was realized by impregnation of 0.50 g of SiO_2 in PEI solution under strong stirring. In a first step, the SiO_2 was introduced into PEI aqueous solution with different concentrations (from 200 $mg.L^{-1}$ to 2 $g.L^{-1}$) under stirrer during 9 hours, at 25°C and an initial pH solution close to 10.4. Thereafter, the effect of pH solution and temperature on the adsorption of PEI onto silica was investigated for pH ranging from 5 to 12 and temperatures between 25 and 50°C, using a PEI solution with an initial concentration of 1 $g.L^{-1}$. To finish, the material stability was evaluated during desorption tests with distilled water (pH ~ 6), for temperatures between 25 and 50°C.

2.2. Tested pollutants: methylene blue and lead

Methylene blue ($C_{16}H_{18}ClN_3S$) is a cationic dye with molecular mass of 373.9 $g.mol^{-1}$. Its adsorption has long been used to assess the performance of activated carbon before its use in water

purification plants. It is recognized for its usefulness to characterize adsorbent materials and strongly adsorbs onto solids such as silica gel [29,30]. In this study, we used methylene blue of analytical grade from Merck company (Germany). Synthetic dye solutions were prepared by dissolving weighted amount of methylene blue (noted MB) in distilled water. As PEI, the concentrations of MB were measured by spectrophotometry, using the UV-visible spectrophotometry at a maximum wavelength of 580 nm.

Lead solution was prepared from Lead (II) nitrate reagent ≥ 99% salt (Aldrich) in nitric acid solution at 1% (v/v). Subsequently, dilute solutions were prepared by dissolving a given volume of lead solution in distilled water to obtain the required concentrations (between 10 and 50 $mg.L^{-1}$). Lead analysis is performed using a PinAAcle 900T atomic absorption spectrometer, requiring an air/acetylene mixture (PERKIN-ELMER) at 283.3 nm. The sensibility of this device is about 1% (0.01 A).

2.3. Characterization methods

2.3.1. FTIR spectroscopy

Fourier transform infrared spectroscopy was used to identify the functional groups in the samples. Silica samples, before and after chemical modification, were analyzed with a Tensor 27 FTIR spectrophotometer in the wavenumber range, between 400 and 4000 cm^{-1}, using KBr beam splitter under ambient conditions.

2.3.2. SEM (Scanning Electron Microscopy) analysis

An environmental scanning electron microscope in High Vacuum mode (FEI Quanta 250) equipped with an X-Ray detector and operating at an accelerating voltage of 10 kV was used to determine the elementary composition of the adsorbents and observe their surface morphology.

Each sample has been covered with two thin layers of gold to increase its conductivity and put on a double-sided conductive tape, itself placed on a metal stub.

2.3.3. XPS analysis

X-ray photoelectron spectroscopy was used to determine the chemical composition of the geothermal silica before and after modification. XPS measurements were conducted on an AXIS Ultra DLD Detector spectrometer (Kratos) equipped with a hemispherical electron analyzer and Al Kα (1253.6 eV) X-ray exciting source.

2.3.4. BET (Brunauer, Emmett and Teller) method

The BET surface area and porous properties were determined by nitrogen adsorption experiments, using a Micromeritics model ASAP-2020 analyzer. The sample was degassed for 24 hours to remove all of the physisorbed species on the surface of the adsorbent before measurement of the nitrogen adsorption-desorption isotherms at 77 K. Surface area was calculated by using the BET equation [31] and the pore size distribution was estimated using the Barrett–Joiner–Halenda (BJH) model [32], during the desorption phase.

2.4. Adsorption experiments

Adsorption experiments were carried out in a shaking thermostatic water bath under various initial pollutant concentrations, adsorbent dosage, pH and temperature values. The pH solution was adjusted by the addition of NaOH or HCl solution under magnetic stirring.

For MB kinetic adsorption studies, 15 mg of adsorbent was mixed with MB solutions at initial concentrations ranging from 10 to 50 $mg.L^{-1}$, for different pH (2 - 10) and temperature (25 - 45°C) conditions. For the Pb kinetic adsorption studies, three adsorbent dosages (1 g, 0.5 g and 0.25 g) were introduced in Pb solution at initial concentration of 50 $mg.L^{-1}$, for different pH (4 - 7) and temperature (25 - 45°C) conditions. To monitor the concentration of MB or Pb solutions over time,

a few milliliters of the sample stored in the water bath was taken with a syringe, filtered, and analyzed, using a UV/visible spectrophotometer or atomic absorption spectrometer. Each experiment was repeated three times.

The amount of pollutant adsorbed per mass unit of adsorbent at time q ($mg.g^{-1}$) was calculated using Eq. (1):

$$q=\frac{(C_i-C_t)}{m}V \qquad (1)$$

where C_i is the initial concentration ($mg.L^{-1}$), C_t is the concentration at time t ($mg.L^{-1}$), V is the volume of the solution (L) and m is the mass of adsorbent (g).

To determinate the MB adsorption isotherm, 15 g of adsorbent was placed in contact with the solution at different concentrations (10 - 120 $mg\text{-}L^{-1}$), at pH 10 and at 25°C. For Pb adsorption isotherm, 0,50 g of adsorbent was placed in contact with the solution at different concentrations (10 - 50 $mg\text{-}L^{-1}$), at pH 5 and at 25°C. Then, MB and Pb concentrations were measured at time t = *0*then at the end of the test when the equilibrium is reached.

2.5. Sorption modeling in batch system

2.5.1. Adsorption kinetic models

In order to investigate the adsorption mechanisms, two kinetic models, the Lagergren first-order and the pseudo-second order, have been exploited to analyze the experimental data.

The pseudo-first-order kinetic model Lagergren [33] relates the adsorption rate to the metal adsorbed amount at time t as:

$$log(q_e - q_t) = logq_e - \frac{k_1 \cdot t}{2.303} \qquad (2)$$

where q_e and q_t ($mg.g^{-1}$) are the adsorbed amounts at equilibrium and at time t, respectively; and k_1 (min^{-1}) is the pseudo-first-order rate constant. The slope of the plot of $log\ (q_e - q_t)$ vs. t indicates the k_1 value.

The pseudo-second-order kinetic model [34] may be written in the form:

$$\frac{t}{q_t} = \frac{1}{k_2 q_e^2} + \frac{t}{q_e} \qquad (3)$$

where k_2 (g.mg^{-1}.min^{-1}) is the pseudo-second-order rate constant. The slope and the intercept of the plot of t/q_t vs. t allow to determinate q_e and k_2 values respectively.

2.5.2. Adsorption isotherm

The equilibrium between adsorbed molecules onto adsorbent materiel (q_e) and molecules in solution (C_e) at a constant temperature have been described using four adsorption isotherms: Langmuir [35], Freundlich [36], Redlich-Peterson [37] and Brouers-Sotolongo [38] models (Table 1).

Table 1

Adsorption isotherm models tested.

Model	Expression q_e	Linear form
Langmuir	$\frac{q_m \cdot K_L \cdot C_e}{1 + K_L \cdot C_e}$ (4)	$\frac{1}{q_e} = \frac{1}{q_m \cdot K_L} \cdot \frac{1}{C_e} + \frac{1}{q_m}$ (5)
Freundlich	$K_F \cdot C_e^{1/n}$ (6)	$\ln q_e = \ln K_F + \frac{1}{n} \cdot \ln C_e$ (7)
Redlich-Peterson	$\frac{A \cdot C_e}{\left(1 + K_{RP} \cdot C_e^{\beta}\right)}$ (8)	$\ln\left(\frac{A \cdot C_e}{q_e} - 1\right) = \beta \cdot \ln(C_e) + \ln K_{RP}$ (9)
Brouers-Sotolongo	$q_{BS}\left(1 - exp\left(-K_{BS} C_e^{\alpha_{BS}}\right)\right)$ (10)	

where q_e (mg.g^{-1}) is the adsorption capacity in equilibrium, C_e (mg.L^{-1}) is the equilibrium concentration, K_L (L.mg^{-1}) is the Langmuir adsorption constant related to energy of adsorption, q_m (mg/g) indicates the maximum adsorption capacity, K_F (mg/g(L/mg)$^{1/n}$) is Freundlich constant, n is the Freundlich intensity parameter representing the favorability of the sorption system, K_{RP} is the Redlich–Peterson isotherm constant (L.g^{-1}), A is the Redlich–Peterson isotherm constant ((L.mg^{-1})$^{\beta}$) and β is the Redlich– Peterson exponent (dimensionless), q_{BS} (mg/g) is the saturation value, K_{BS}

(L/mg) is the Brouers-Sotolongo constant, and the exponent α_{BS} (dimensionless) is a measure of the width of the sorption energy distribution and therefore of the energy heterogeneity of the surface.

2.5.3. Error estimation

In this study, the correlation coefficient R^2 (determined from non-linear analysis) and the average absolute percentage deviation, %D (Eq. (11)) were used to estimate the goodness of the studied models:

$$\%D = \left(\frac{1}{N}\sum_{i=1}^{N}\left|\frac{q_{e_{exp}} - q_{e_{cal}}}{q_{e_{exp}}}\right|\right) * 100 \qquad (11)$$

where N is the number of experimental data points, $q_{e_{cal}}$ is the theoretically calculated adsorption capacity at equilibrium and $q_{e_{exp}}$ is the experimental adsorption capacity at equilibrium.

3. Results

3.1. Selection of PEI/SiO_2 material

The first adsorption experiments of PEI on geothermal silica were carried out using a solution of PEI at 1 $g.L^{-1}$ for pH ranging from 5 to 12 and at room temperature, 25°C.

Results show that the adsorption capacity increases with pH and the maximum adsorption capacity is reached at pH 12 (Fig. 2). At the high pH values, electrostatic interactions between PEI and SiO_2 at the solid/liquid interface are higher due to the increased ionization of the hydroxyl groups on the surface of SiO_2 [39]. Additional tests were conducted at pH 12 for temperatures ranging from 25 to 50°C, and using 1 $g.L^{-1}$ PEI solution. The results show that the PEI adsorption onto SiO_2 is favored at low temperature (T = 25°C), indicating an exothermic reaction.

Thereafter, adsorption experiments were conducted under optimum pH and temperature conditions (pH 12 and T = 25°C) at different PEI initial concentrations between 0.200 and 2 $g.L^{-1}$. Fig. 3 shows that the amount of PEI adsorbed onto SiO_2 surface increases with increasing initial

concentration of PEI solution. Under those experimental conditions, the grafting rate of PEI varied between approximately 4.1 and 8.9%. In order to control the stability of the elaborated materials, desorption tests in distilled water (pH ~ 6) were conducted, according to the same protocol as the adsorption tests. Fig. 4 shows that the material was relatively stable with a desorbed fraction of less than 4% of the adsorbed fraction. A detailed observation of the desorption process as a function of time reveals that the release of the PEI takes place immediately after the introduction of the material into the distilled water. Subsequently, the desorbed fraction is partially re-adsorbed and the desorbed fraction remains unchanged.

These experiments allow to conclude that, at 25°C and pH 12, the material obtained by introducing SiO_2 in a solution of PEI at 1 $g.L^{-1}$ (7.4% grafting rate) had the best ratio of adsorbed fraction/desorbed fraction. This material has therefore been characterized and used to lead the adsorption tests for the two studied pollutants.

3.2. Characterization of SiO_2 and PEI/SiO_2 materials

Silica was characterized before and after PEI adsorption by SEM microscopy, FTIR and X-ray photoelectron spectroscopies and nitrogen absorption method.

The SEM analysis shows that the surface morphology of SiO_2 seems rather porous and has a roughness with granular and friable aspects (Fig. S1a). After PEI adsorption, no significant modification of the surface morphology of the silica is observable (Fig. S1b). Porous materials can be characterized in terms of pore size distribution derived from gas sorption data, and IUPAC [40] proposes a classification of adsorption isotherms that reflects the relationship between porous structures and their sorption type. In the context of physi-sorption, pores can be classified according to their size (less than 2 nm as microporous, from 2 nm to 50 nm as mesoporous, and greater than 50 nm as macro-porous) and their adsorption isotherms into six types (Type I to VI). The pore size distributions for the adsorbents (SiO_2 and PEI/SiO_2) obtained by N_2 adsorption-desorption isotherms at 77 K are shown in Fig. 5. Table 2 compares the pore characteristics deduced from

these curves (volumes of micro-, meso-, and macro-pores) and specific areas, for SiO_2 and PEI/SiO_2 materials.

Table 2

Specific surface (S_{BET}) and pore characteristics of SiO_2 and PEI/SiO_2 materials deduced from the N_2 adsorption–desorption isotherms: V_{micro},V_{meso} and V_{tot} are volumes of micro-, meso-, and macro-pores respectively and $Ø_{pore}$ the medium diameter.

	S_{BET} ($m^2.g^{-1}$)	V_{micro} ($cm^3.g^{-1}$)	V_{meso} ($cm^3.g^{-1}$)	V_{tot} ($cm^3.g^{-1}$)	$Ø_{pore}$ (Å)
SiO_2	207	0.017	1.23	1.24	189
PEI/SiO_2	184	0.018	1.15	1.17	198

Fig. 5 shows that the adsorption isotherms are characteristic of meso-porous adsorbents (type IV), which corresponds to an initial mono/multilayer adsorption on the meso-pores followed by condensation of the pores. These curves also reveal the presence of hysteresis loops (type H1), parallel and almost vertical adsorption and desorption branches, generally observed in the case of adsorbents having a very narrow range of uniform meso-pores. The pore size distribution shows that for both materials, the average pore diameter is in the order of 200 Å, and the meso-porosity is between 100 and 450 Å. Table 2 shows that grafted PEI onto silica surface leads to a slight decrease of specific surface area (from 206 $m^2.g^{-1}$ to 184 $m^2.g^{-1}$) and a slight decrease of the meso-pores volume too (from 1.23 $cm^3.g^{-1}$ to 1.15 $cm^3.g^{-1}$). This evolution, reported by other authors [41,42] is caused by pore obstruction of the largest meso-pores by PEI molecules. Nevertheless, meso-pore volume of PEI/SiO_2 material remains sufficiently high to allow the adsorption of other pollutant molecules.

The infrared spectrums of SiO_2, PEI/SiO_2 and PEI materials are shown in Fig. 6. After grafting PEI onto SiO_2, the O-H bands at 972 and 800 cm^{-1} are shifted and are less intense. Furthermore, the spectrum of the PEI/SiO2 composite exhibits, in addition to the hydroxyl functions associated with the silicic support, peaks common to the spectrum of the liquid PEI, confirming its grafting on the

surface of the silica. Indeed, adsorption bands corresponding to the vibration of N-H bond of the primary amines appear at 3400 and 1633 cm^{-1}, and the absorption peaks at 1473 and 1571 cm^{-1} are characteristic of the C─N bond. The appearances of these absorption bands show that PEI macromolecules have been grafted onto silica surface, and PEI/SiO_2 particles have been formed.

X-ray photoelectron spectroscopy was also used to study the changes in the chemical composition of the silica surface after PEI grafting. The recorded spectra are given in Fig. 7. The spectrum of SiO_2 presents the main peaks corresponding to silica composition, namely O1s at 532.7 eV and Si2p at 103.3 eV. After PEI grafting, an additional N1s nitrogen peak at 398.5 eV is observed. Table 3 shows that, for SiO_2, the Si:O atomic ratio is 25.4:60.1 and for PEI/SiO_2, the Si:O:N atomic ratio is 21.9:53.5:5.3. The presence of 5% of nitrogen in the elemental composition of PEI/SiO_2 confirms the PEI grafting onto silica surface.

Table 3

Atomic compositions determined by XPS for SiO_2 and PEI/SiO_2. The peak of carbon observed is due to an accidental contamination of the sample by the residual fumes in the analytical chamber.

	Si	O	N	C
SiO_2	25.4	60.1	-	14.5
PEI/SiO_2	21.9	53.5	5.3	18.8

For SiO_2, the oxygen peak O1s breaks down into two signals at 532.6 and 533.7 eV, which respectively reflect the presence of (Si-O/O-H) groups and the absorption of H_2O water molecules on silica surface. The Si 2p spectrum shows a peak at 103.3 eV indicating that Si atoms are bound only to oxygen atoms (SiO_2 form) (See Supplementary information: Fig. S2a). After PEI grafting, the N1s core-level spectrum shows three peaks at 398.4, 399.6 and 400.9 eV attributed to N in the =N−, NH and NH_3^+ respectively (See Supplementary information: Fig. S2b). The charged form would result from the interaction of the amine function with the silanol groups on the surface of the silica.

3.3. Adsorption of lead

3.3.1. Adsorption of lead (Pb^{2+}) onto SiO_2 and PEI/SiO_2

SiO_2 and PEI/SiO_2 materials were brought into contact with a lead solution of 50 $mg.L^{-1}$ during 6 hours in order to investigate the adsorption kinetic of lead on these materials, and to assess the PEI grafting effect on the lead adsorption capacity. The experiments were carried out at pH 5 (*i.e.* without pH adjusting) and 25°C. Fig. 8 shows the adsorption kinetic curves obtained for both materials. The amount of lead adsorbed increases with time and reach equilibrium in 2 and 3 hours for SiO_2 and PEI/SiO_2, respectively. At equilibrium, the PEI/SiO_2 adsorption capacity is about 18 $mg.g^{-1}$ whereas SiO_2 adsorption capacity is about 5.3 $mg.g^{-1}$. Consequently, the PEI grafting significantly improved the geothermal silica ability for lead adsorption. This result is consistent with the observations of Aguado et al. [16], reporting a difficulty to adsorb metal compounds directly onto untreated silica, despite their porous structure well adapted to adsorption processes.

As PEI grafting significantly improves the adsorption capacity of lead on geothermal silica, we have focused on PEI/SiO_2 material in the study of pH effects and adsorption models presented below.

3.3.2. Influence of pH on lead adsorption on PEI/SiO_2

The effect of pH on lead adsorption on PEI/SiO_2 was investigated for pH ranging from 4 to 7. At pH higher than 7, lead species hydrolyzed and subsequently the precipitation of lead hydroxide species occurred [43]. Fig. 9 shows that the adsorption capacity of lead increases with the pH into the investigated pH range. This can be attributed to an increase of the number of negatively charged groups on the adsorbent surface with increasing pH, which leads to higher adsorption of Pb^{2+}. At equilibrium, q = 11.40, 22.05 and 25.77 $mg.g^{-1}$, at pH 4, 5 and 7 respectively.

3.4. Adsorption of methylene blue (MB)

3.4.1. Adsorption of MB onto SiO_2 and PEI/SiO_2

The adsorption capacity of methylene blue (MB) on SiO_2 and PEI/SiO_2 composite was investigated, using MB initial concentrations between 10 and 50 $mg.L^{-1}$, and adsorbent dosage between 5 and 20 mg. The experiment was carried out at 25°C and the pH value of the MB solution was close to 10. Fig. 10 shows that the adsorption capacities of both adsorbents towards MB increase with MB initial concentrations and on the other hand, they are not influenced by the adsorbent dosage. Under identical experimental conditions, SiO_2 adsorption capacity is at least 2 times higher than that of PEI/SiO_2. This behavior suggests that on PEI/SiO_2 surface, there is no interaction between PEI and MB, which means that only the active sites available on the surface of silica are involved in the process of MB adsorption.

Since PEI grafting does not improve the adsorption ability of silica for MB, therefore, we focused on SiO_2 for the rest of the study on MB adsorption.

3.4.2. Influence of pH solution on MB adsorption on SiO_2

The effect of pH solution on SiO_2 adsorption capacity of MB was investigated for pH ranging from 2 to 10 at 25°C. Fig. 11 shows that the adsorption capacity increases with increasing pH. The adsorption capacity at equilibrium is minimal at pH 2 and 4, with q values smaller than 4 $mg.g^{-1}$ and maximal at pH 10, with $q \backsim 108$ $mg.g^{-1}$. This behavior can be explained by the fact that in acidic solution, the silica surface is overall neutral (pH_{pzc} = 2.5), thus the actives adsorption sites are limited [44]. In alkaline solutions, the presence of OH^- ions leads to deprotonation of the silanol group onto silica surface. The silica surface becomes negatively charged and thereafter the MB molecules, which are positively charged, can be more easily adsorbed.

4. Data interpretation and discussion

4.1. Adsorption of lead

4.1.1. Adsorption kinetics of PEI/SiO_2 for Pb^{2+}

In order to model the adsorption kinetics of lead (II) ions, two kinetic models, the pseudo-first-order and pseudo-second-order (see details in section 2.5), have been applied to the experimental data obtained for the different adsorbent dosages (1 g, 0.5 g and 0.25 g) (Fig. S3). The kinetic parameters are given in Table 4. It appears that adsorption kinetics could be well explained by the pseudo-second-order model since the computed correlation coefficients R^2 are closer to 1 for this model. These results suggest that the chemisorption might be the rate-limiting step that controls the adsorption process [34].

Table 4

Pseudo-first and pseudo-second order model parameters for lead adsorption on PEI/SiO_2, for the three investigated adsorbent dosages (0.25, 0.5 and 1 g).

Mass of adsorbent (g)	0.25	0.50	1
Pseudo-first order			
k_1 (min^{-1})	0.010	0.014	0.012
q_e ($mg.g^{-1}$)	12.74	15.75	15.03
R^2	0.9332	0.9748	0.9572
%D	63.698	41.056	55.206
Pseudo-second order			
k_2*10^{-2} ($g.mg^{-1}.min^{-1}$)	0.21	0.16	0.17
q_e ($mg.g^{-1}$)	25.71	23.81	27.10
R^2	0.9983	0.9996	0.9997
%D	4.900	2.380	2.189
q_e experimental ($mg.g^{-1}$)	24.15	21.81	25.21

4.1.2. Adsorption isotherms of Pb^{2+} on PEI/SiO_2

In order to understand the adsorption mechanism, experimental data were fitted using the Langmuir, Freundlich, Redlich-Peterson and Brouers-Sotolongo isotherm models (Fig. 12). The isotherm model parameters are listed in Table 5. Redlich-Peterson model is the best model to describe the adsorption of lead (II) on PEI/SiO_2 (R^2 = 0.999 and %D = 0.933). With a value of β close to 1 (β = 0.96) the experimental isotherm is approaching the Langmuir isotherm. The maximum adsorption capacity (q_{max}) of adsorbent calculated from Langmuir isotherm equation, 26.9 $mg.g^{-1}$, corresponds to the total capacity of the adsorbent for lead (II) ions. These results involve a monolayer sorption and a homogeneous distribution of active sites on the PEI/SiO_2 surface.

Table 5

Langmuir, Freundlich, Redlich-Peterson and Brouers-Sotolongo constants for the adsorption of lead (II) on PEI/SiO_2.

Isotherms	Parameters	Data
Langmuir	q_m ($mg.g^{-1}$)	26.9
	K_L ($L.mg^{-1}$)	2.39
	R^2	0.9886
	%D	4.569
Freundlich	K_F ($mg/g(L/mg)^{1/n}$)	16.56
	n	5.95
	R^2	0.9848
	%D	5.167
Redlich-Peterson	A [$(L.mg^{-1})^{\beta}$]	106.82
	K_{RP} ($L.g^{-1}$)	4.99
	β	0.92
	R^2	0.9990
	%D	0.933
Brouers-Sotolongo	q_{max} ($mg.g^{-1}$)	28.15
	K_{BS} ($L.mg^{-1}$)	0.93
	α	0.41
	R^2	0.9963
	%D	2.232

To evaluate the effectiveness of the PEI/SiO_2 materiel studied compared to other adsorbents used to remove lead from aqueous solutions, a comparison was made on the basis of the Langmuir adsorption capacity q_m. Table 6 shows that the adsorption capacity of our composite (q_m ~ 27 $mg.g^{-1}$) is comparable to values observed in most of the previously studied adsorbents (18 - 59 $mg.g^{-1}$), except for activated carbon derived from biomass plants and PEI-modified biomass which present a q_m values ten times higher (~ 200 - 280 $mg.g^{-1}$). Moreover, two of these studies with lead on modified silica, with thiol and PEI, [45,46] present adsorption capacities (17,8 and 17.6 $mg.g^{-1}$) lower than our experimental value.

Table 6

Adsorption capacities of different adsorbents for lead removal. AC: activated carbon.

Adsorbent	pH	q_m ($mg.g^{-1}$)	Reference
Functionalized silica gel. thiol	5.5	17.8	[45]
PEI/SiO_2 composite	6	17.6	[46]
AC prepared from coconut shell	4.5	26.5	[4]
PEI/SiO_2 composite	**5**	**26.9**	**This study**
AC originating from cow bone	4	47.6	[47]
Sugarcane bagasse/carbon nanotube composite	4.5	53.1 - 58.6	[48]
PEI-modified biomass	5.5	204.3	[49]
AC prepared from biomass plant	5	279.7	[50]

4.2. Adsorption of methylene blue (MB)

4.2.1. Thermodynamic parameters

Methylene blue adsorption onto SiO_2 was studied for an initial concentration of 50 $mg.L^{-1}$ at pH 10 and for temperatures between 25 and 45°C. The thermodynamic parameters were determined from the kinetic data obtained at different temperatures. Thus, Gibbs free energy ΔG° ($kJ.mol^{-1}$), enthalpy ΔH° (kJ. mol^{-1}) and entropy ΔS° (J. $mol^{-1}.K^{-1}$) were calculated using Eqs (12) and (13):

$$\Delta G° = -RT\ lnK \qquad (12)$$

$$lnK = \frac{\Delta S°}{R} - \frac{\Delta H°}{RT} \qquad (13)$$

with *K* the equilibrium constant, *R* the ideal gas constant (J.(mol K)$^{-1}$) and *T* the absolute temperature (K).

The negative value found for ΔG° (- 3.66 kJ.mol^{-1}) suggests that the adsorption process is spontaneous at 25°C. The negative value of ΔH° (- 2.81 kJ.mol^{-1}) indicates the adsorption of SiO_2 towards methylene blue is an exothermic process and the low enthalpy value corresponds to physical interaction between MB and silica surface [51]. The positive value of ΔS° (2.83 J.mol^{-1}.K^{-1}) suggests that entropy increases in the solid-liquid interface due to a favorable adsorption process.

4.2.2. Modeling of MB adsorption kinetics on SiO_2

In order to evaluate adsorption dynamics, the pseudo-first-order and the pseudo-second-order kinetic models were applied to fit our experimental data, obtained

for the different initial MB concentration (10 to 50 mg.L^{-1}), at 25°C and pH 10 (Fig. S4). The calculated parameters associated to these kinetic models are given in Table 7. Results show that the pseudo-second order is the best model to predict the kinetic of MB adsorption onto SiO_2. Indeed, on the one hand this model presents the highest correlation coefficients R^2 and the weakest error deviations %D. On the other hand, the calculated adsorption capacities q_e are close to the experimental values whatever the initial MB concentration. This suggests an adsorption of MB molecules on SiO_2 by chemisorption.

Table 7

Pseudo-first and pseudo-second order parameters for MB adsorption onto SiO_2.

Initial concentration (mg.L^{-1})	10	20	30	40	50
q_e experimental (mg.g^{-1})	12.38	31.77	50.43	68.03	42.55
Pseudo-first order					
k_1 (min^{-1})	0.18	0.11	0.04	0.006	0.05
q_e (mg.g^{-1})	11.09	23.05	14.26	15.39	43.35
R^2	0.9884	0.9793	0.7752	0.7287	0.9207
%D	0.801	2.111	5.518	5.952	0.145
Pseudo-second order					

k_2 (g.mg^{-1}. min^{-1})	-0.05	0.13	0.01	0.002	0.06
q_e (mg.g^{-1})	12.52	32.15	51.02	68.03	44.05
R^2	0.9996	0.9997	0.9999	0.9992	0.9952
%D	0.136	0.098	0.074	0.838	0.682

4.2.3. Adsorption isotherms of MB on SiO_2

In order to better understand the adsorption processes and estimate the maximal adsorption capacity, the equilibrium data of MB adsorption onto SiO_2, at 25°C and pH 10, were modeled using Langmuir, Freundlich, Redlich-Peterson and Brouers-Sotolongo isotherm models (Fig. S5). The calculated parameters for these isotherm models are given in Table 8. The best fit is obtained for Redlich-Peterson isotherm (R^2 = 0.997 and %D = 2.82). For this model, the computed β value is equal to 1 which means that this isotherm is close to Langmuir isotherm. The low value of K_L *(i.e.* 0.28) suggests a high affinity of raw silica for the MB molecules through a monolayer sorption and a homogeneous distribution of active sites on SiO_2 surface. The correlation coefficient R^2 close to 1 and the low deviation error %D found for Brouers-Sotolongo isotherm (0.994 and 3.33 respectively) indicate that this model is also in good agreement with the experimental data. This last model enables to estimate a maximal adsorption capacity of MB onto SiO_2 around 100 mg.g^{-1} , at pH 10 and 25°C.

Table 8

Langmuir, Freundlich, Redlich-Peterson and Brouers-Sotolongo parameters calculated for the adsorption of MB onto SiO_2.

Isotherms	Parameters	
Langmuir	q_m (mg.g^{-1})	107.65
	K_L (L.mg^{-1})	0.28
	R^2	0.994
	%D	4.14
Freundlich	K_F (mg/g(L/mg)$^{1/n}$)	44.27
	n	4.88
	R^2	0.914

	%D	14.43
Redlich-Peterson	K_{RP} ($L.g^{-1}$)	0.18
	A [$(L.mg^{-1})^{\beta}$]	25.33
	β	1
	R^2	0.997
	%D	2.82
Brouers-Sotolongo	q_{max} ($mg.g^{-1}$)	100.36
	K_{BS} ($L.mg^{-1}$)	0.26
	α	0.82
	R^2	0.995
	%D	3.33

To evaluate the effectiveness of the geothermal silica compared to other adsorbents usually proposed to remove methylene blue from aqueous solutions, a comparison with published data was made on the basis of the calculated Langmuir adsorption capacity q_m. The results reported in Table 9 show that the adsorption capacity of the studied materials is well correlated with the specific surface area., The silica and silica-based composites materials are between the best performing adsorbents. With a notable capacity of about 108 $mg.g^{-1}$, the Bouillante geothermal silica, investigated in this study, could be considered as an effective adsorbent material for the removal of methylene blue in aqueous solutions.

Table 9

Adsorption capacity q_m (derived from Langmuir model) of different adsorbents for MB removal. S_{BET} is the specific surface.

Adsorbent	q_m ($mg.g^{-1}$)	S_{BET} ($m^2.g^{-1}$)	Reference
Rice biomass	8.2	0.47	[52]
Diatomite treated with sodium hydroxide	27,9	15,9	[53]
Date palm leaves	43.1	-	[54]
Kaolin and zeolite	45/22	61.1/24.5	[55]
Geothermal silica (SiO_2)	**107.64**	**207**	**This study**
Magnesium silicate (84% de SiO_2)	144.9	250	[56]
Graphene	153.8	295.5	[57]
Composite CTAB/TEOS (SiO_2 source)	285.7	1423	[58]

5. Conclusion

The dissolved silica precipitated during the exploitation of geothermal fluids is generally considered as a waste product and remain mostly unused. Very few studies have been conducted on this abundant geothermal silica as a byproduct of electricity production through its use in innovative absorbent materials. So, in this study, the possibility to use the silica extracted from the Bouillante geothermal water as an adsorbent of pollutants contaminating natural waters has been investigated. Unmodified and modified SiO_2 materials have been tested using two pollutants: methylene blue and lead at different initial concentrations, and under various pH and temperature conditions.

Unmodified geothermal silica (SiO_2) shows very interesting adsorption capacity for methylene blue. The maximum adsorption capacity q_m = 108 $mg.g^{-1}$ is obtained at the higher investigated pH (pH =10) and at the lower investigated temperature (T = 25°C). The thermodynamic study has revealed that the adsorption process is spontaneous and exothermic. The equilibrium data could be modeled by the Redlich-Peterson and Langmuir isotherms, that suggesting a monolayer sorption and a homogeneous distribution of active sites on the silica surface. The adsorption kinetic follows a pseudo-second-order model. Moreover, the characterization of silica materials shows that the raw geothermal silica is easily modifiable. In this study, the grafting of PEI onto SiO_2 surface has allowed a substantial improvement of its adsorption capacity for removing lead (II). The maximum adsorption capacity (q_m = 27 $mg.g^{-1}$) was obtained at pH 7 and 25°C for PEI/SiO_2 material. The equilibrium data could be modeled by the Redlich-Peterson and Langmuir isotherms suggesting a monolayer sorption and a homogeneous distribution of active sites on PEI/SiO_2 surface. The adsorption kinetic follows a pseudo-second-order model.

To resume, raw geothermal silica has showed interesting adsorption capacity values for methylene blue, especially at high pH values whereas for lead adsorption, coating of silica by using PEI is a necessary step to obtain an interesting adsorption capacity.

According to the promising results obtained in this study, geothermal silica from Bouillante geothermal water could be used for the elaboration of new adsorbents necessary for the treatment of naturel waters. These geothermal silica-based absorbents can be as efficient as activated carbon (AC) commonly used but with lower economic and environmental costs if geothermal silica is available locally and large quantities can be extracted from geothermal waters. Additionally, the use of geothermal precipitates of potential commercial values could provide a way to reduce the cost of exploitation of geothermal energy resources and help to its development.

Acknowledgements

The authors wish to thank Geothermie Bouillante compagny for having authorized us to access to the Bouillante geothermal plant and the staff for their welcome and help during sampling. We also thank the C3MAG laboratory (University of Antilles) for their assistance in characterizing the studied absorbent material through MEB, TEM, and DRX analysis.

References

[1] Y.-M. Cabidoche, R. Achard, P. Cattan, C. Clermont-Dauphin, F. Massat, J. Sansoulet, Long-term pollution by chlordecone of tropical volcanic soils in the French West Indies: A simple leaching model accounts for current residue, Environ. Pollut. 157 (2009) 1697–1705. doi:10.1016/j.envpol.2008.12.015.

[2] G. Crini, Recent developments in polysaccharide-based materials used as adsorbents in wastewater treatment, Prog. Polym. Sci. 30 (2005) 38–70. doi:10.1016/j.progpolymsci.2004.11.002.

[3] B.L. Morris, A.R.L. Lawrence, P.J.C. Chilton, B. Adams, R.C. Calow, B.A. Klinck, Groundwater and its susceptibility to degradation: a global assessment of the problem and options for management, United Nations Environment Programme, 2003.

[4] M. Sekar, V. Sakthi, S. Rengaraj, Kinetics and equilibrium adsorption study of lead(II) onto activated carbon prepared from coconut shell, J. Colloid Interface Sci. 279 (2004) 307–313. doi:10.1016/J.JCIS.2004.06.042.

[5] Z.A. Ghani, M.S. Yusoff, N.Q. Zaman, M.F.M.A. Zamri, J. Andas, Optimization of preparation conditions for activated carbon from banana pseudo-stem using response surface methodology on removal of color and COD from landfill leachate, Waste Manag. 62 (2017) 177–187. doi:10.1016/J.WASMAN.2017.02.026.

[6] M. Danish, T. Ahmad, S. Majeed, M. Ahmad, L. Ziyang, Z. Pin, S.M. Shakeel Iqubal, Use of banana trunk waste as activated carbon in scavenging methylene blue dye: Kinetic, thermodynamic, and isotherm studies, Bioresour. Technol. Reports. 3 (2018) 127–137. doi:10.1016/J.BITEB.2018.07.007.

[7] S. Gaspard, S. Altenor, E.A. Dawson, P.A. Barnes, A. Ouensanga, Activated carbon from vetiver roots: Gas and liquid adsorption studies, J. Hazard. Mater. 144 (2007) 73–81. doi:10.1016/J.JHAZMAT.2006.09.089.

[8] H.G. Svavarsson, S. Einarsson, A. Brynjolfsdottir, Adsorption applications of unmodified geothermal silica, Geothermics. 50 (2014) 30–34. doi:10.1016/J.GEOTHERMICS.2013.08.001.

[9] O.G.M. Sandoval, G.C.D. Trujillo, A.E.L. Orozco, Amorphous silica waste from a geothermal central as an adsorption agent of heavy metal ions for the regeneration of industrial pre-treated wastewater, Water Resour. Ind. 20 (2018) 15–22. doi:10.1016/J.WRI.2018.07.002.

[10] B. Sanjuan, P. Jousset, G. Pajot-Métivier, N. Debeglia, M. de Michele, M. Brach, F. Dupont, G. Braibant, E. Lasne, F. Duré, Monitoring of the Bouillante Geothermal Exploitation (Guadeloupe, French West Indies) and the Impact on Its Immediate Environment, 2010.

[11] M.A. H. Serra, B. Sanjuan, Modélisation géochimique des risques de dépôts minéraux au cours de l'exploitation des forages géothermiques de Bouillante (Guadeloupe), Report BRGM/RP-53154-FR, 2004.

[12] D.L. Gallup, F. Sugiaman, V. Capuno, A. Manceau, Laboratory investigation of silica removal from geothermal brines to control silica scaling and produce usable silicates, Appl. Geochemistry. 18 (2003) 1597–1612. doi:10.1016/S0883-2927(03)00077-5.

[13] R.T. Harper, J.H. Johnston, N. Wiseman, Controlled precipitation of amorphous silica from geothermal fluids or other aqueous media containing silicic acid, 1997. doi:10.1016/0375-6505(93)90007-A.

[14] A. Maimoni, Minerals recovery from salton sea geothermal brines: a literature review and proposed cementation process, Geothermics. 11 (1982) 239–258. doi:10.1016/0375-6505(82)90031-1.

[15] C. Dixit, M.-L. Bernard, B. Sanjuan, L. André, S. Gaspard, Experimental study on the kinetics of silica polymerization during cooling of the Bouillante geothermal fluid (Guadeloupe, French West Indies), Chem. Geol. 442 (2016) 97–112. doi:10.1016/j.chemgeo.2016.08.031.

[16] J. Aguado, J.M. Arsuaga, A. Arencibia, M. Lindo, V. Gascón, Aqueous heavy metals removal by adsorption on amine-functionalized mesoporous silica, J. Hazard. Mater. 163 (2009) 213–221. doi:10.1016/J.JHAZMAT.2008.06.080.

[17] A.M. Liu, K. Hidajat, S. Kawi, D.Y. Zhao, A new class of hybrid mesaporous materials with functionalized organic monolayers for selective adsorption of heavy metal ions, Chem. Commun. 0 (2000) 1145–1146. doi:10.1039/b002661l.

[18] L. Bois, A. Bonhommé, A. Ribes, B. Pais, G. Raffin, F. Tessier, Functionalized silica for heavy metal ions adsorption, Colloids Surfaces A Physicochem. Eng. Asp. 221 (2003) 221–230. doi:10.1016/S0927-7757(03)00138-9.

[19] I.P. Blitz, J.P. Blitz, V.M. Gun'ko, D.J. Sheeran, Functionalized silicas: Structural characteristics and adsorption of Cu(II) and Pb(II), Colloids Surfaces A Physicochem. Eng. Asp. 307 (2007) 83–92. doi:10.1016/J.COLSURFA.2007.05.016.

[20] M.N. Ahmed, R.N. Ram, Removal of basic dye from waste-water using silica as adsorbent, Environ. Pollut. 77 (1992) 79–86. doi:10.1016/0269-7491(92)90161-3.

[21] S. Lantenois, B. Prélot, J.-M. Douillard, K. Szczodrowski, M.-C. Charbonnel, Flow microcalorimetry: Experimental development and application to adsorption of heavy metal cations on silica, Appl. Surf. Sci. 253 (2007) 5807–5813. doi:10.1016/J.APSUSC.2006.12.064.

[22] M. Karnib, A. Kabbani, H. Holail, Z. Olama, Heavy Metals Removal Using Activated Carbon, Silica and Silica Activated Carbon Composite, Energy Procedia. 50 (2014) 113–120. doi:10.1016/J.EGYPRO.2014.06.014.

[23] T.L. Rodrigues Mota, A.P. Marques de Oliveira, E.H.M. Nunes, M. Houmard, Simple process for preparing mesoporous sol-gel silica adsorbents with high water adsorption capacities, Microporous Mesoporous Mater. 253 (2017) 177–182. doi:10.1016/J.MICROMESO.2017.07.010.

[24] N. Chiron, R. Guilet, E. Deydier, Adsorption of Cu(II) and Pb(II) onto a grafted silica:

isotherms and kinetic models, Water Res. 37 (2003) 3079–3086. doi:10.1016/S0043-1354(03)00156-8.

[25] M. Najafi, Y. Yousefi, A.A. Rafati, Synthesis, characterization and adsorption studies of several heavy metal ions on amino-functionalized silica nano hollow sphere and silica gel, Sep. Purif. Technol. 85 (2012) 193–205. doi:10.1016/J.SEPPUR.2011.10.011.

[26] S. Hao, A. Verlotta, P. Aprea, F. Pepe, D. Caputo, W. Zhu, Optimal synthesis of amino-functionalized mesoporous silicas for the adsorption of heavy metal ions, Microporous Mesoporous Mater. 236 (2016) 250–259. doi:10.1016/J.MICROMESO.2016.09.008.

[27] S. Kobayashi, K. Hiroishi, M. Tokunoh, T. Saegusa, Chelating properties of linear and branched poly(ethylenimines), Macromolecules. 20 (1987) 1496–1500. doi:10.1021/ma00173a009.

[28] B.L. Rivas, K.E. Geckeler, Synthesis and metal complexation of poly(ethyleneimine) and derivatives BT - Polymer Synthesis Oxidation Processes, in: Springer, Berlin, Heidelberg, 1992: pp. 171–188. doi:10.1007/3-540-55090-9_6.

[29] M. Rafatullah, O. Sulaiman, R. Hashim, A. Ahmad, Adsorption of methylene blue on low-cost adsorbents: A review, J. Hazard. Mater. 177 (2010) 70–80. doi:10.1016/J.JHAZMAT.2009.12.047.

[30] R. Saeed, F. Uddin, S. Summer, Adsorption of Methylene Blue on Activated Charcoal, Asian J. Chem. 17 (2005) 737–742.

[31] E.P. Barrett, L.G. Joyner, P.P. Halenda, The Determination of Pore Volume and Area Distributions in Porous Substances. I. Computations from Nitrogen Isotherms, J. Am. Chem. Soc. 73 (1951) 373–380. doi:10.1021/ja01145a126.

[32] S. Brunauer, P.H. Emmett, E. Teller, Adsorption of gases in multimolecular layers, J. Am. Chem. Soc. 60 (1938) 309–319.

[33] Lagergren, S. K., About the Theory of So-called Adsorption of Soluble Substances, Sven. Vetenskapsakad. Handingarl. 24 (1898) 1–39. https://ci.nii.ac.jp/naid/10016440244/

(accessed January 22, 2019).

[34] Y. Ho, G. McKay, Pseudo-second order model for sorption processes, Process Biochem. 34 (1999) 451–465. doi:10.1016/S0032-9592(98)00112-5.

[35] I. Langmuir, The adsorption of gases on plane surfaces of glass, mica and platinium., J. Am. Chem. Soc. 40 (1918) 1361–1403. doi:10.1021/ja02242a004.

[36] H. Freundlich, Kapillarchemie, Akademische verlagsgesellschaft mbh, 1909.

[37] O. Redlich, D.L. Peterson, A Useful Adsorption Isotherm, J. Phys. Chem. 63 (1959) 1024–1024. doi:10.1021/j150576a611.

[38] F. Brouers, O. Sotolongo, F. Marquez, J.P. Pirard, Microporous and heterogeneous surface adsorption isotherms arising from Levy distributions, Phys. A Stat. Mech. Its Appl. 349 (2005) 271–282. doi:10.1016/J.PHYSA.2004.10.032.

[39] B. Gao, P. Jiang, F. An, S. Zhao, Z. Ge, Studies on the surface modification of diatomite with polyethyleneimine and trapping effect of the modified diatomite for phenol, Appl. Surf. Sci. 250 (2005) 273–279. doi:10.1016/J.APSUSC.2005.02.119.

[40] K.S.W. Sing, Reporting physisorption data for gas/solid systems with special reference to the determination of surface area and porosity (Recommendations 1984), Pure Appl. Chem. 57 (1985) 603–619. doi:10.1351/pac198557040603.

[41] M.-L. Delacour, E. Gailliez, M. Bacquet, M. Morcellet, Poly(ethylenimine) coated onto silica gels: Adsorption capacity toward lead and mercury, J. Appl. Polym. Sci. 73 (1999) 899–906. doi:10.1002/(SICI)1097-4628(19990808)73:6<899::AID-APP6>3.0.CO;2-O.

[42] M. Ghoul, M. Bacquet, M. Morcellet, Uptake of heavy metals from synthetic aqueous solutions using modified PEI—silica gels, Water Res. 37 (2003) 729–734. doi:10.1016/S0043-1354(02)00410-4.

[43] P.J. Pretorius, P.W. Linder, The adsorption characteristics of δ-manganese dioxide: a collection of diffuse double layer constants for the adsorption of H+, Cu2+, Ni2+, Zn2+, Cd2+ and Pb2+, Appl. Geochemistry. 16 (2001) 1067–1082. doi:10.1016/S0883-

2927(01)00011-7.

[44] R.K. Iler, The chemistry of silica : solubility, polymerization, colloid and surface properties, and biochemistry, Wiley, 1979.

[45] A.K. Kushwaha, N. Gupta, M.C. Chattopadhyaya, Adsorption behavior of lead onto a new class of functionalized silica gel, Arab. J. Chem. 10 (2017) S81–S89. doi:10.1016/J.ARABJC.2012.06.010.

[46] F. An, B. Gao, Chelating adsorption properties of PEI/SiO2 for plumbum ion, J. Hazard. Mater. 145 (2007) 495–500. doi:10.1016/J.JHAZMAT.2006.11.051.

[47] M.A.P. Cechinel, S.M.A.G. Ulson de Souza, A.A. Ulson de Souza, Study of lead (II) adsorption onto activated carbon originating from cow bone, J. Clean. Prod. 65 (2014) 342–349. doi:10.1016/J.JCLEPRO.2013.08.020.

[48] I.A.A. Hamza, B.S. Martincigh, J.C. Ngila, V.O. Nyamori, Adsorption studies of aqueous Pb(II) onto a sugarcane bagasse/multi-walled carbon nanotube composite, Phys. Chem. Earth, Parts A/B/C. 66 (2013) 157–166. doi:10.1016/J.PCE.2013.08.006.

[49] S. Deng, Y.-P. Ting, Characterization of PEI-modified biomass and biosorption of Cu(II), Pb(II) and Ni(II), Water Res. 39 (2005) 2167–2177. doi:10.1016/J.WATRES.2005.03.033.

[50] Ö. Gerçel, H.F. Gerçel, Adsorption of lead(II) ions from aqueous solutions by activated carbon prepared from biomass plant material of Euphorbia rigida, Chem. Eng. J. 132 (2007) 289–297. doi:10.1016/J.CEJ.2007.01.010.

[51] C.E. James M. Montgomery, Water treatment principles and design, Wiley, 1985. https://catalogue.nla.gov.au/Record/17396 (accessed January 22, 2019).

[52] M.S.U. Rehman, I. Kim, J.-I. Han, Adsorption of methylene blue dye from aqueous solution by sugar extracted spent rice biomass, Carbohydr. Polym. 90 (2012) 1314–1322.

[53] J. Zhang, Q. Ping, M. Niu, H. Shi, N. Li, Kinetics and equilibrium studies from the methylene blue adsorption on diatomite treated with sodium hydroxide, Appl. Clay Sci. 83–84 (2013) 12–16. doi:10.1016/J.CLAY.2013.08.008.

[54] M. Gouamid, M.R. Ouahrani, M.B. Bensaci, Adsorption Equilibrium, Kinetics and Thermodynamics of Methylene Blue from Aqueous Solutions using Date Palm Leaves, Energy Procedia. 36 (2013) 898–907. doi:10.1016/J.EGYPRO.2013.07.103.

[55] K. Rida, S. Bouraoui, S. Hadnine, Adsorption of methylene blue from aqueous solution by kaolin and zeolite, Appl. Clay Sci. 83–84 (2013) 99–105. doi:10.1016/J.CLAY.2013.08.015.

[56] F. Ferrero, Adsorption of Methylene Blue on magnesium silicate: Kinetics, equilibria and comparison with other adsorbents, J. Environ. Sci. 22 (2010) 467–473. doi:10.1016/S1001-0742(09)60131-5.

[57] T. Liu, Y. Li, Q. Du, J. Sun, Y. Jiao, G. Yang, Z. Wang, Y. Xia, W. Zhang, K. Wang, H. Zhu, D. Wu, Adsorption of methylene blue from aqueous solution by graphene, Colloids Surfaces B Biointerfaces. 90 (2012) 197–203. doi:10.1016/J.COLSURFB.2011.10.019.

[58] M. Anbia, S.A. Hariri, Removal of methylene blue from aqueous solution using nanoporous SBA-3, Desalination. 261 (2010) 61–66. doi:10.1016/J.DESAL.2010.05.030.

List of Figures

Figure 1

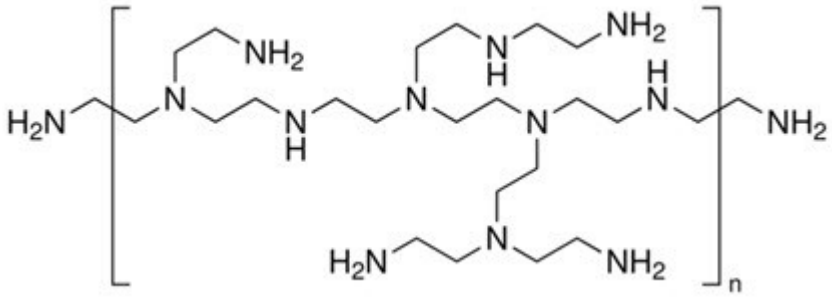

Figure 2

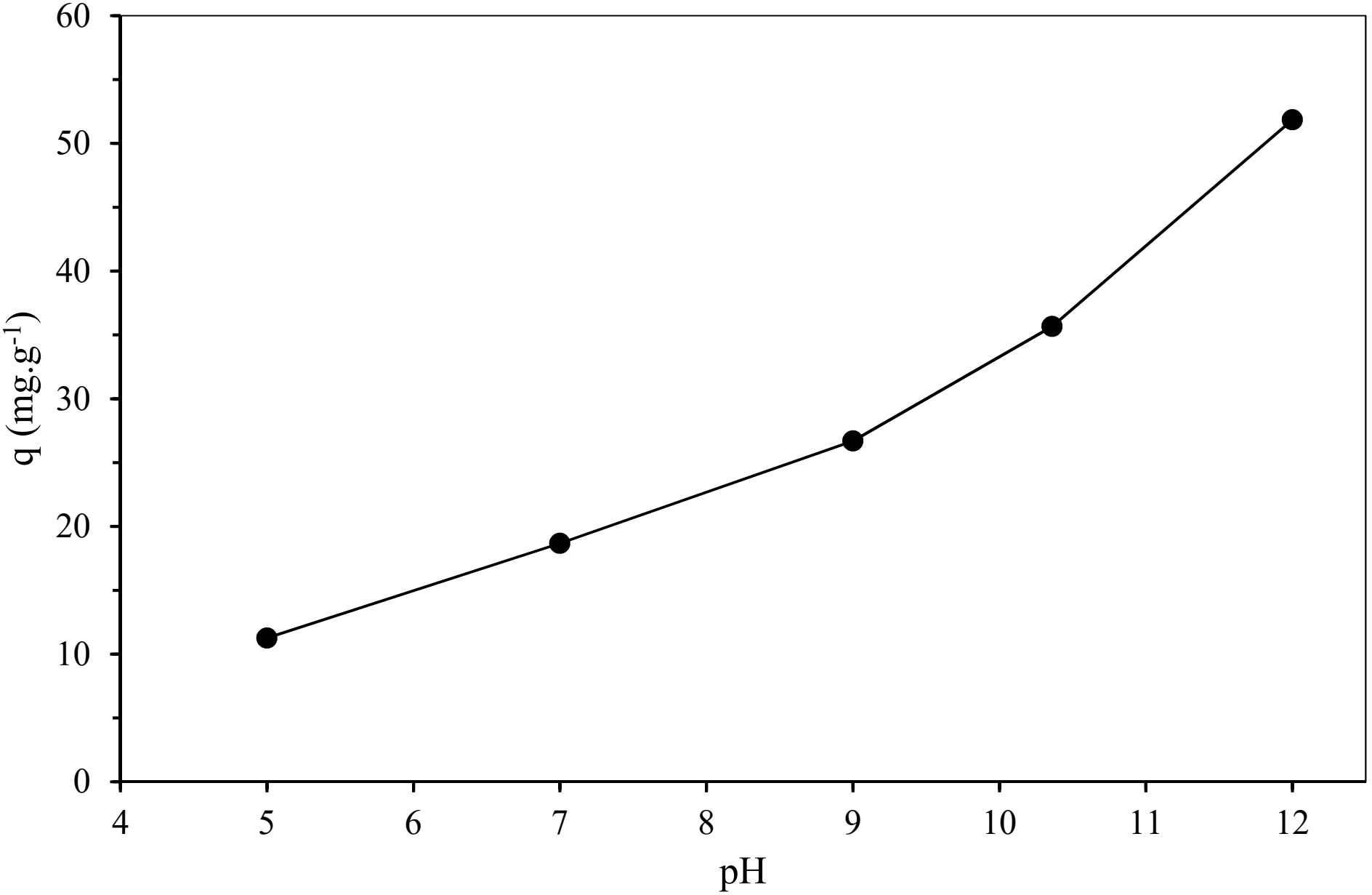

Figure 3

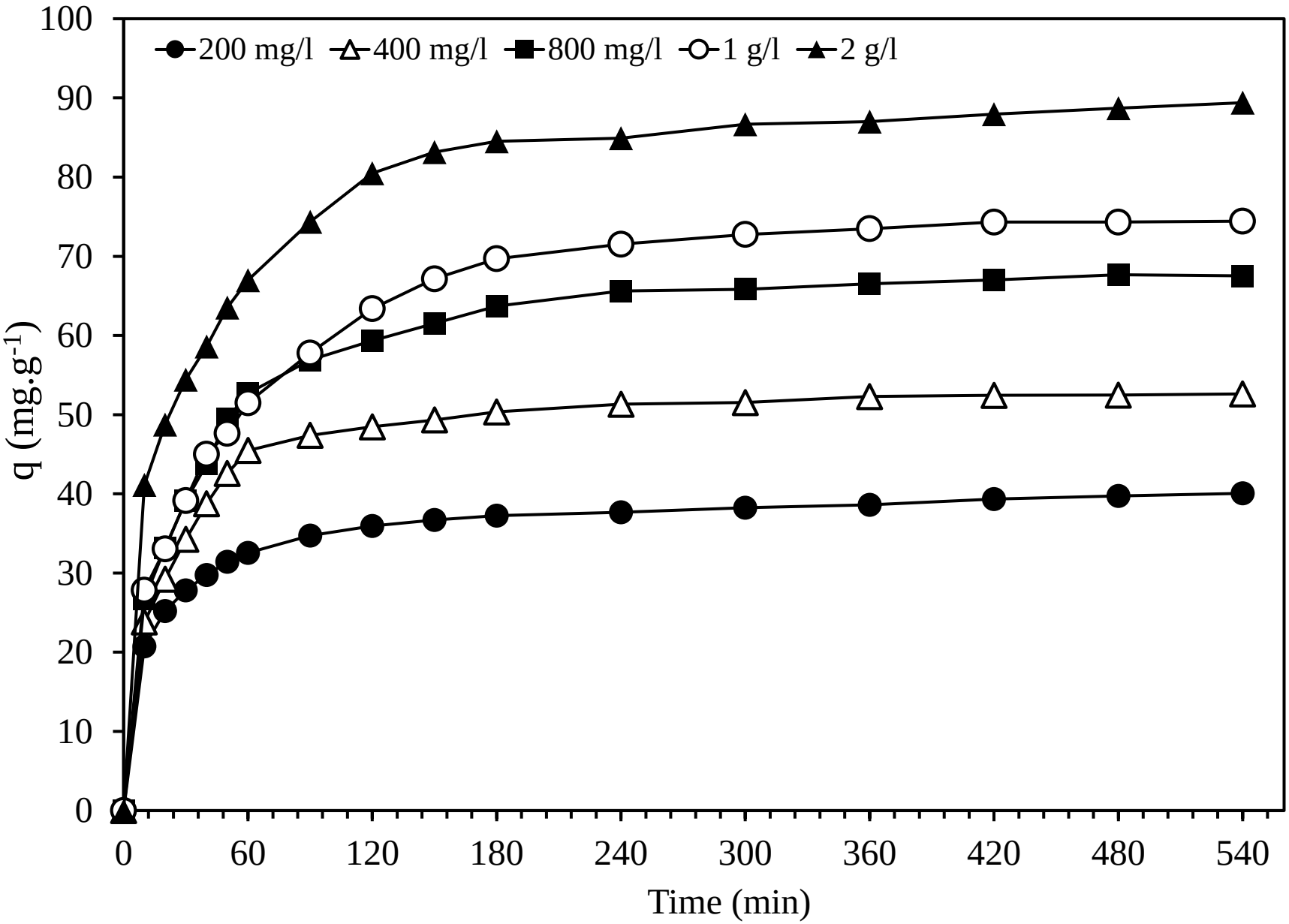
200 mg/l
400 mg/l
800 mg/l
1 g/l
2 g/l
q (mg.g-1)
Time (min)
0
10
20
30
40
50
60
70
80
90
100
0
60
120
180
240
300
360
420
480
540

Figure 4

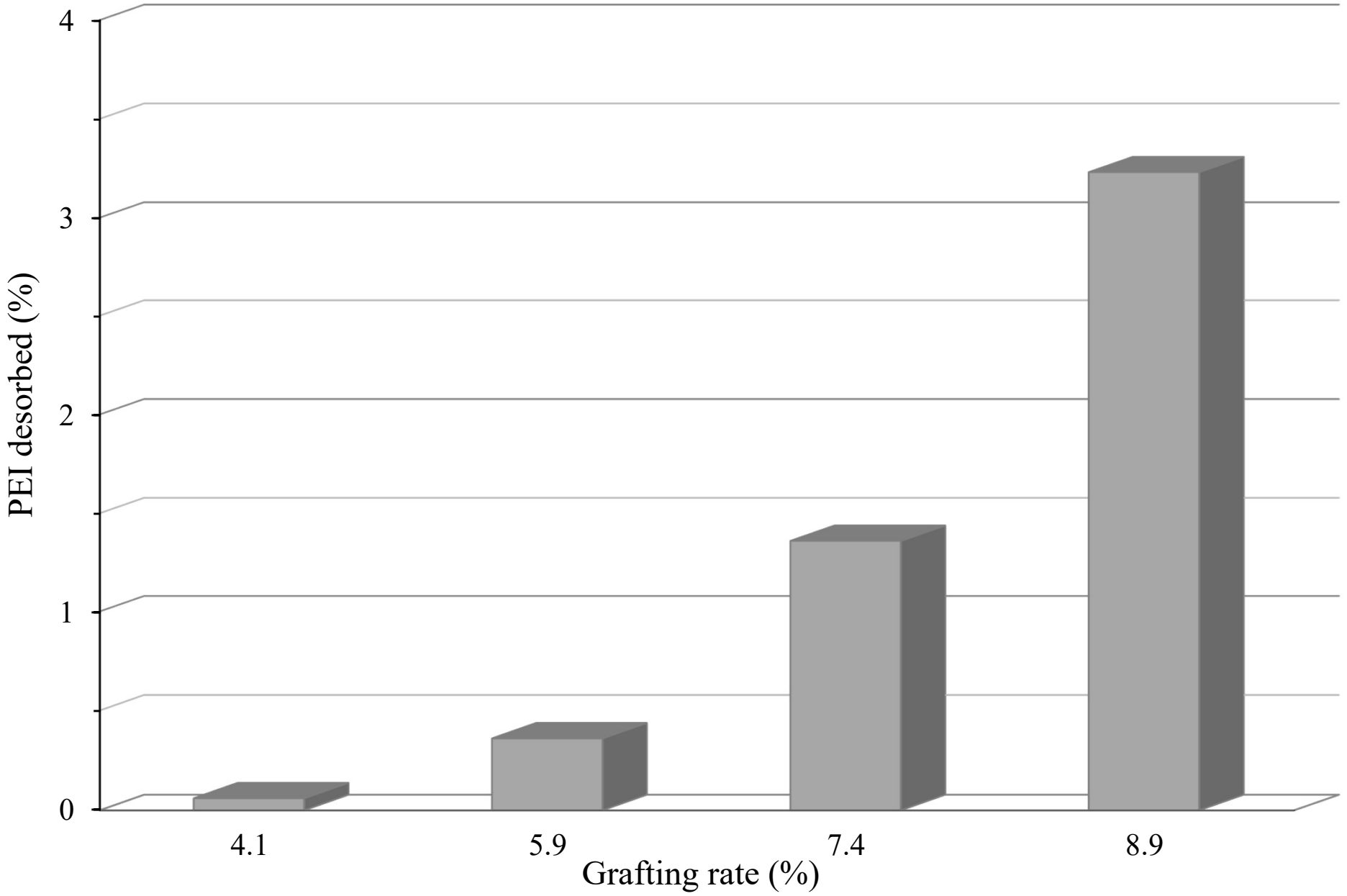

Figure 5

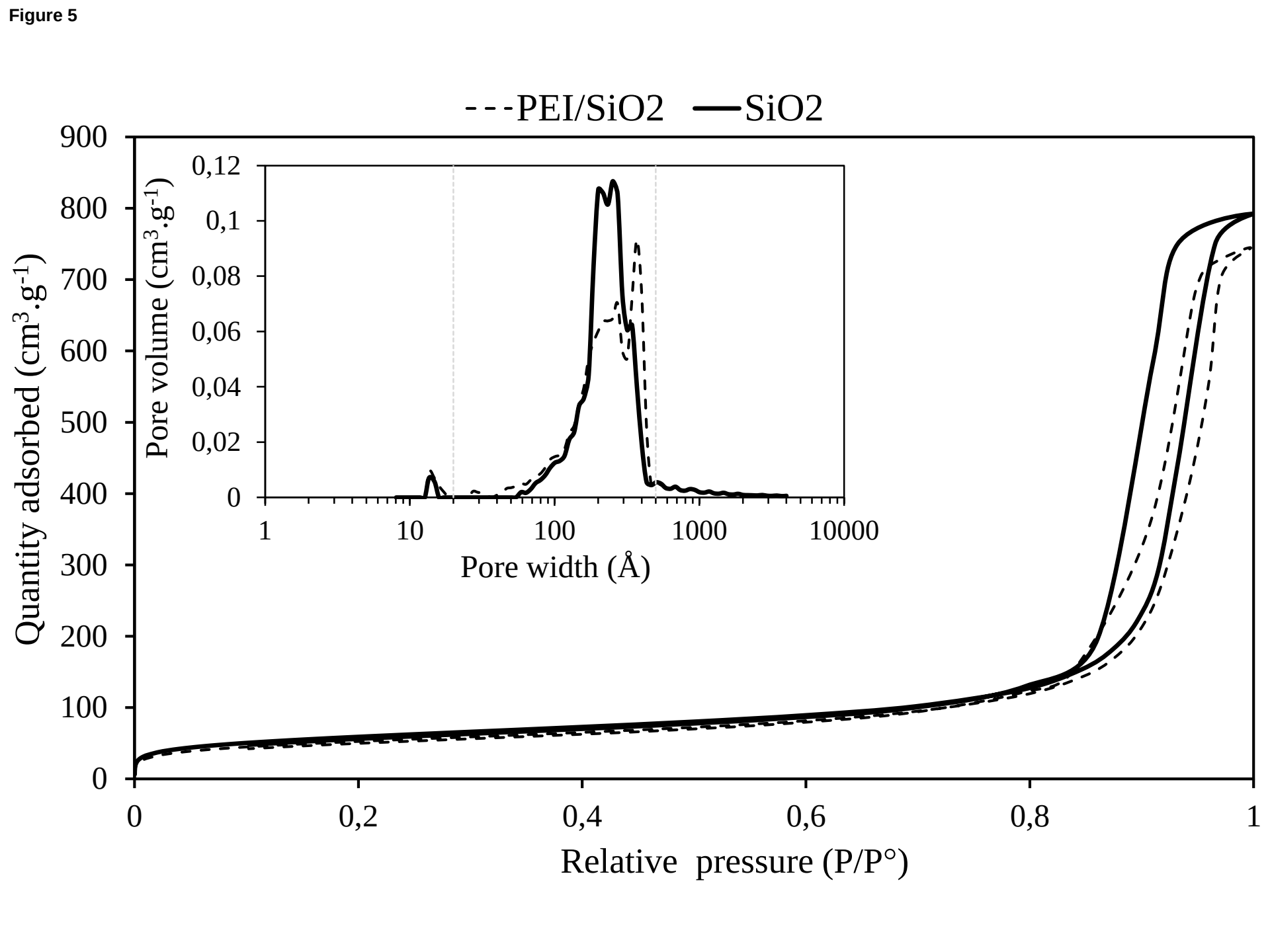
---PEI/SiO2
—SiO2
Quantity adsorbed (cm3.g-1)
900
800
700
600
500
400
300
200
100
0
0
0,2
0,4
0,6
0,8
1
Relative pressure (P/P°)
Pore volume (cm3.g-1)
0,12
0,1
0,08
0,06
0,04
0,02
0
1
10
100
1000
10000
Pore width (Å)

Figure 6

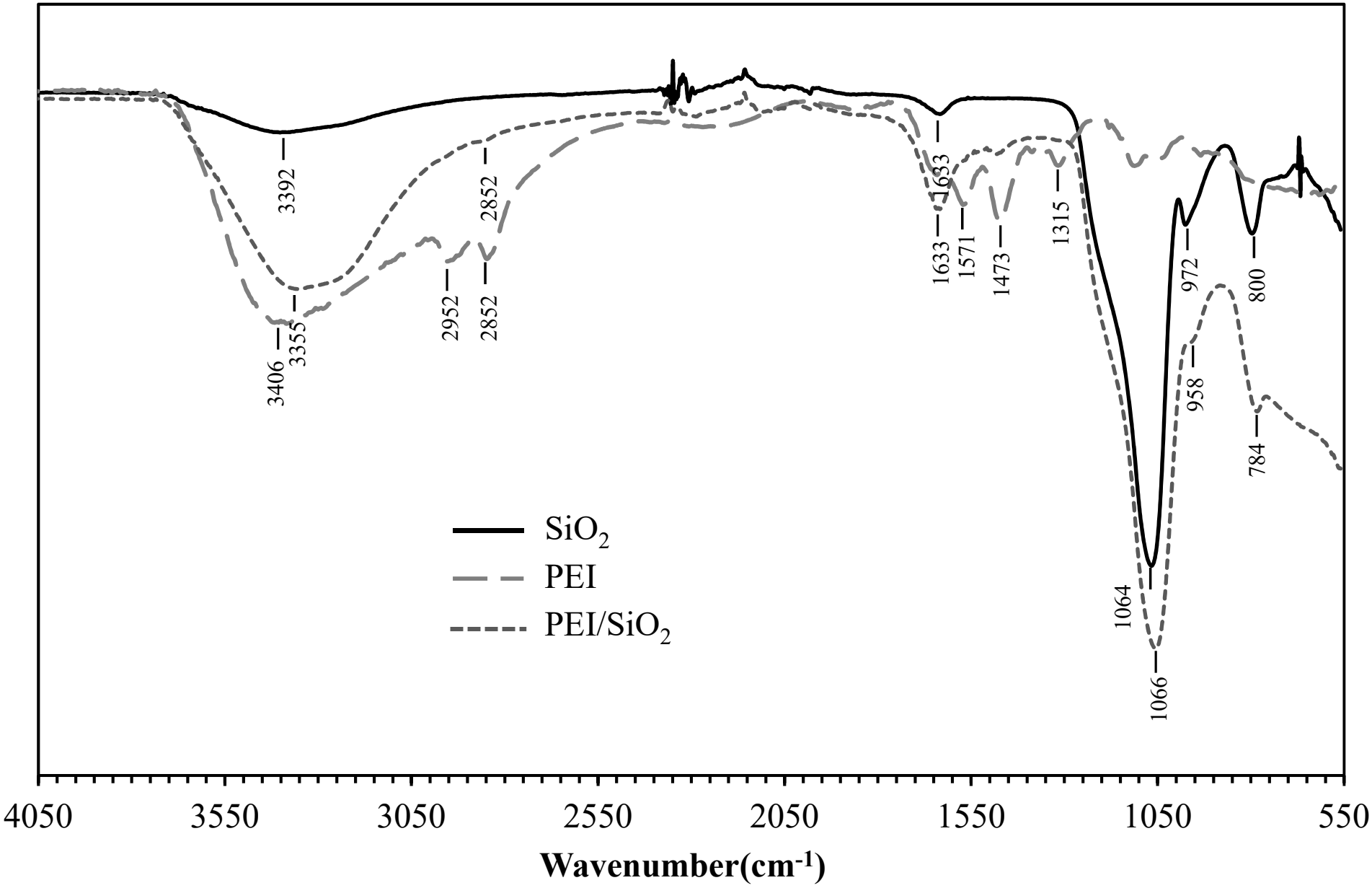
3392
3406
3355
2952
2852
2852
1633
1633
1571
1473
1315
1064
1066
958
972
800
784
SiO2
PEI
PEI/SiO2
4050
3550
3050
2550
2050
1550
1050
550
Wavenumber(cm-1)

Figure 7

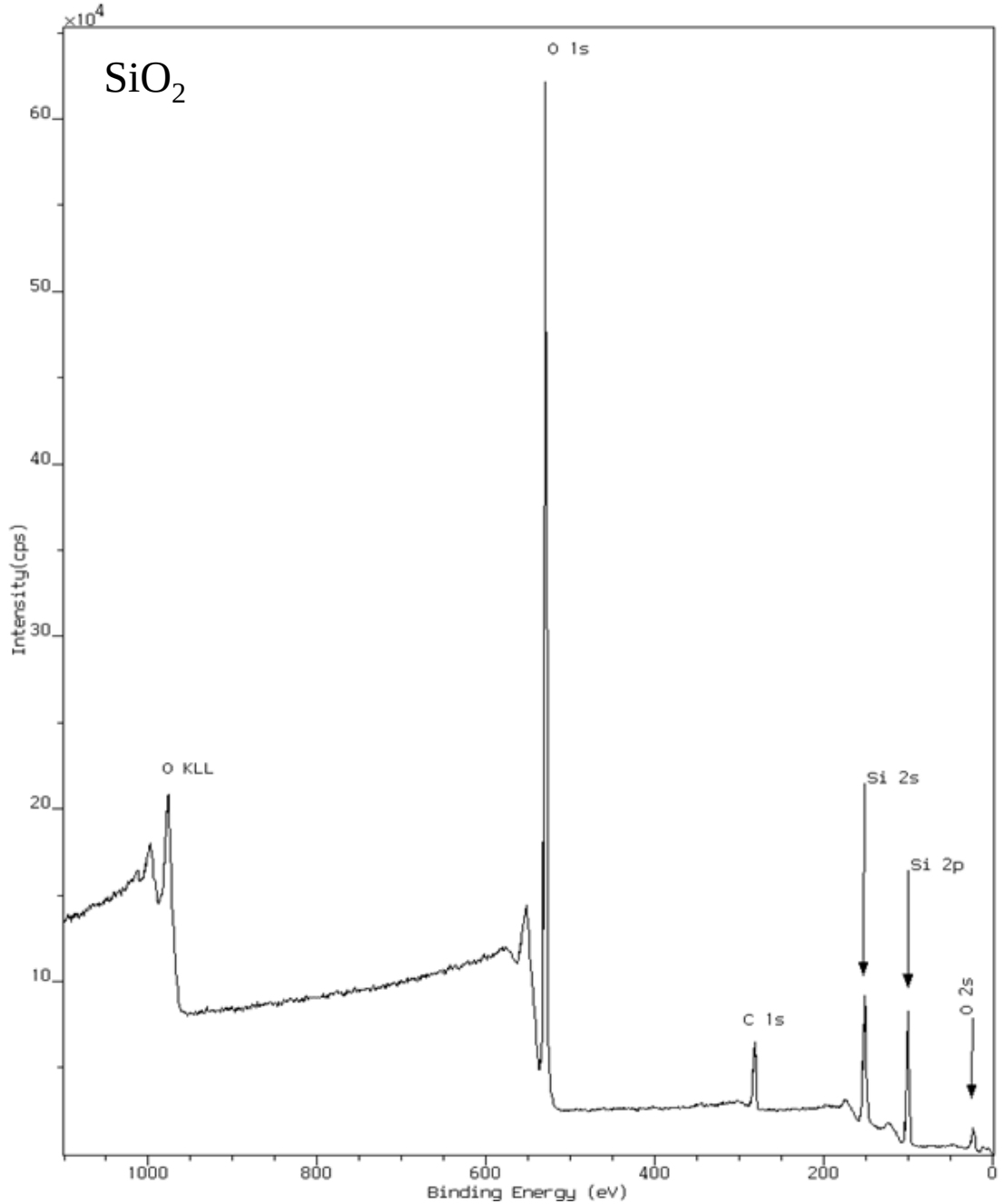
SiO2
×10^4
O 1s
O KLL
C 1s
Si 2s
Si 2p
O 2s
Intensity(cps)
Binding Energy (eV)

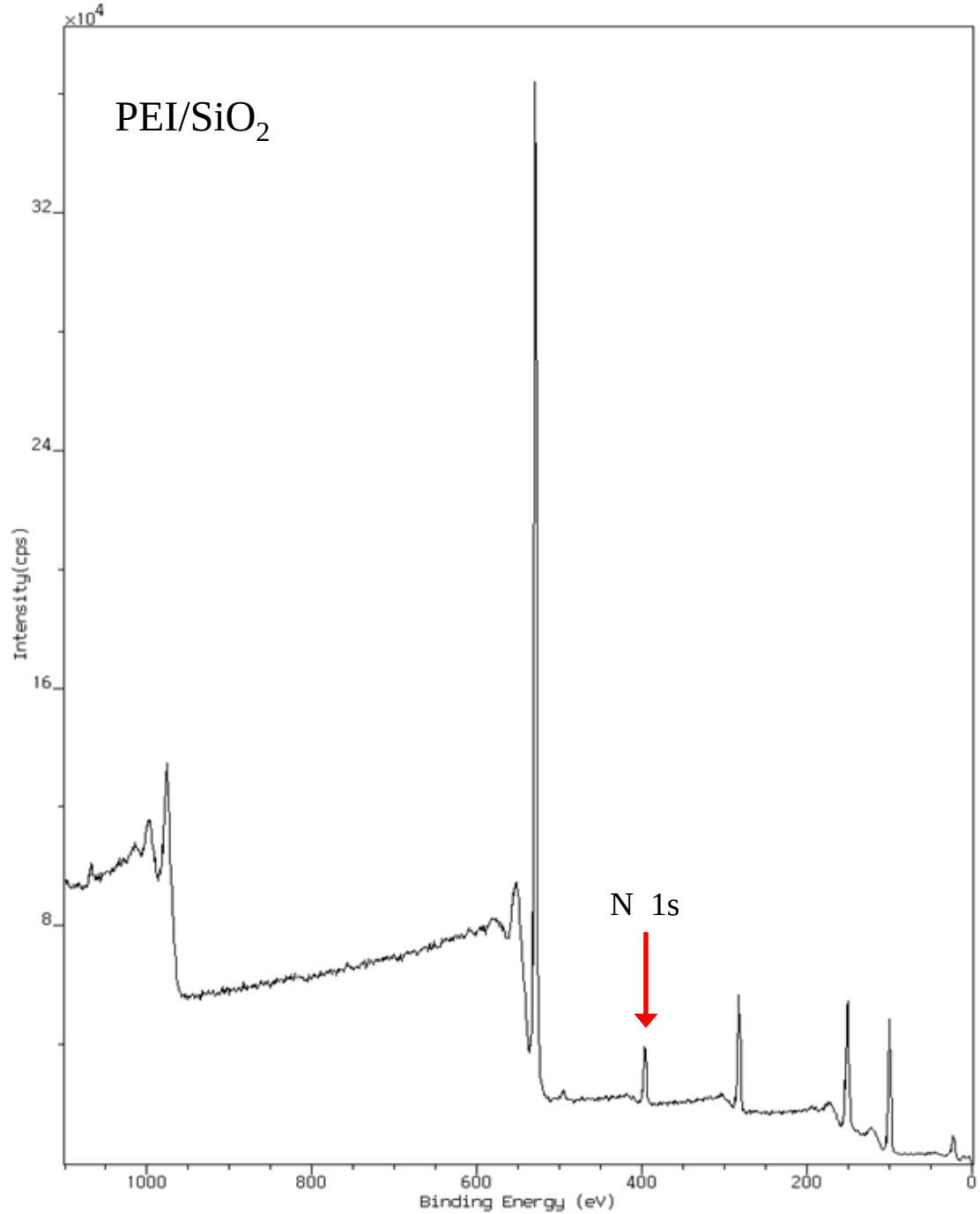
PEI/SiO2
×10^4
N 1s
Intensity(cps)
Binding Energy (eV)

Figure 8

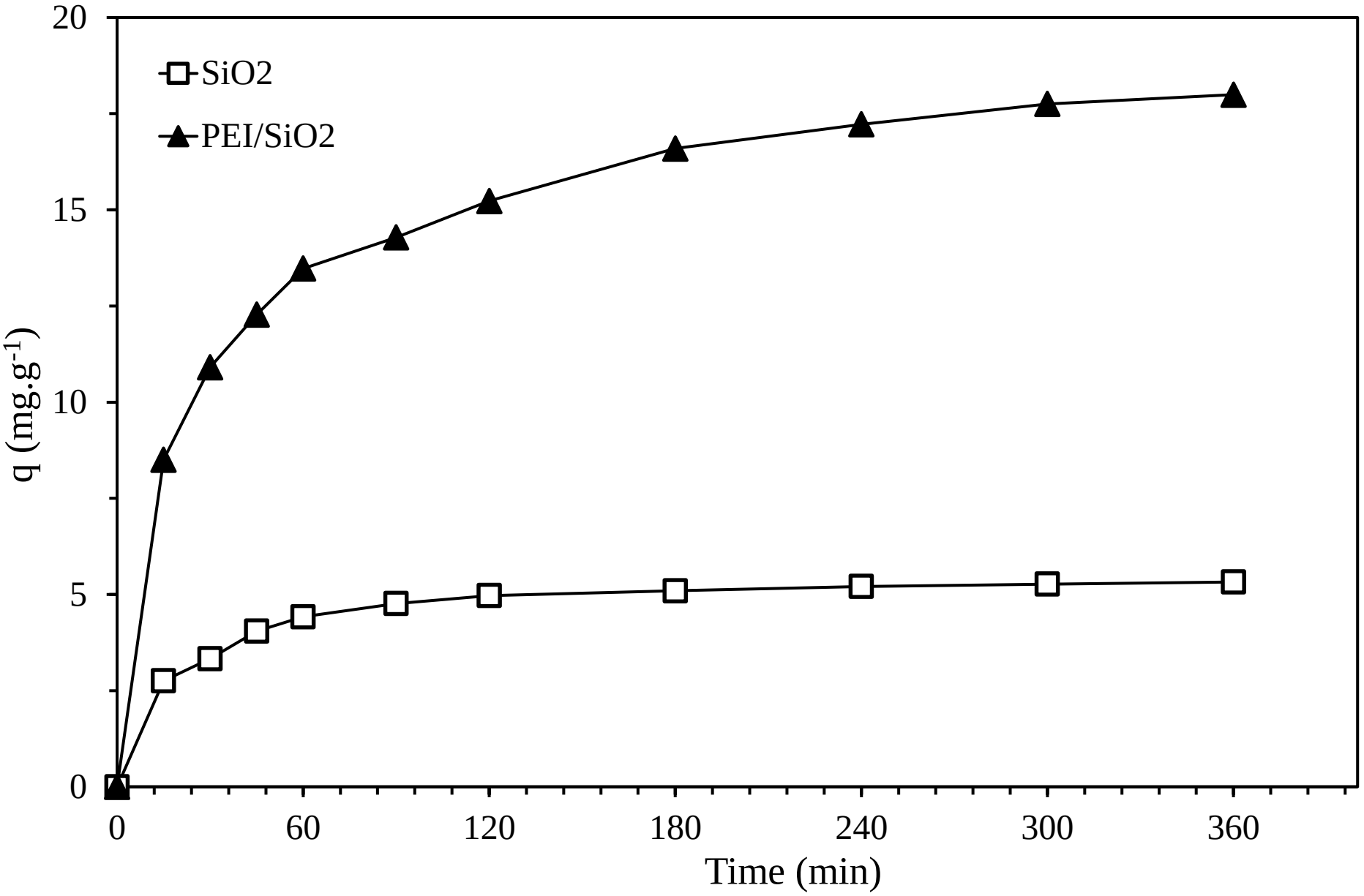

Figure 9

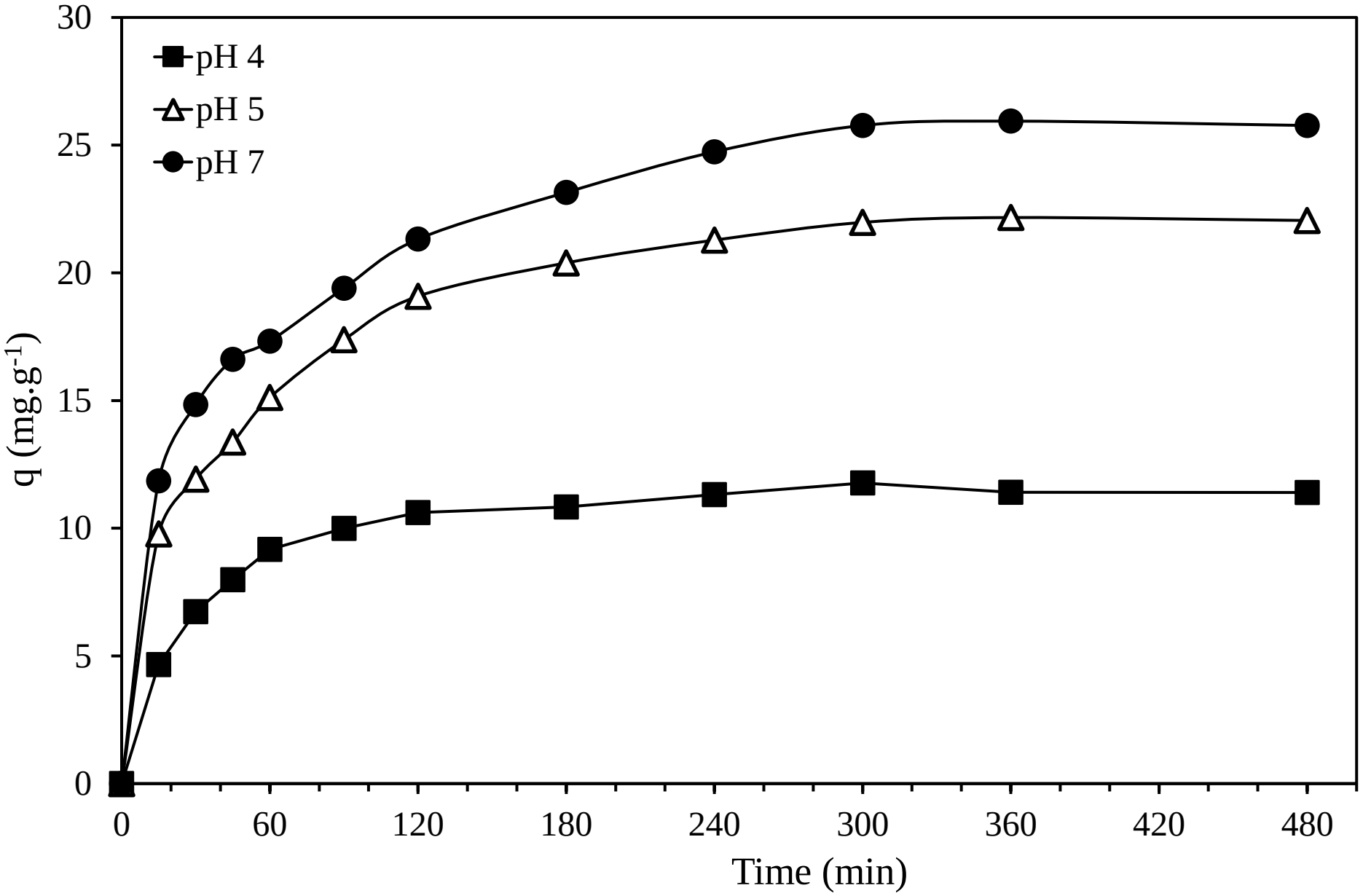
pH 4
pH 5
pH 7
q (mg.g-1)
Time (min)
0
5
10
15
20
25
30
0
60
120
180
240
300
360
420
480

Figure 10

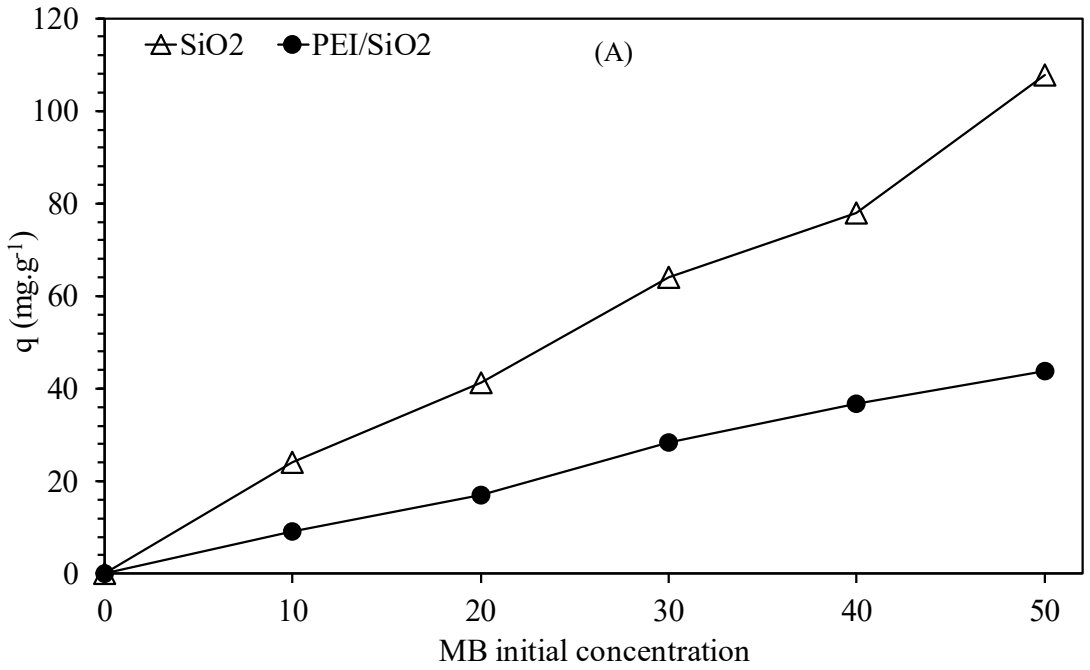
SiO2
PEI/SiO2
(A)
q (mg.g-1)
MB initial concentration
0
20
40
60
80
100
120
0
10
20
30
40
50

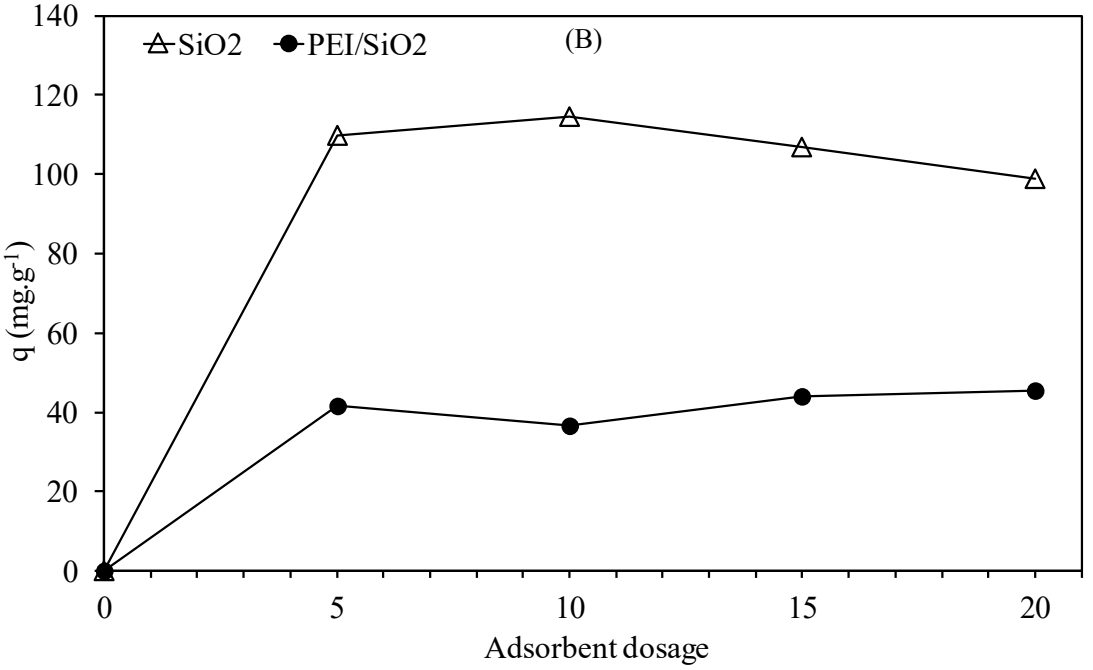
SiO2
PEI/SiO2
(B)
q (mg.g-1)
Adsorbent dosage
0
20
40
60
80
100
120
140
0
5
10
15
20

Figure 11

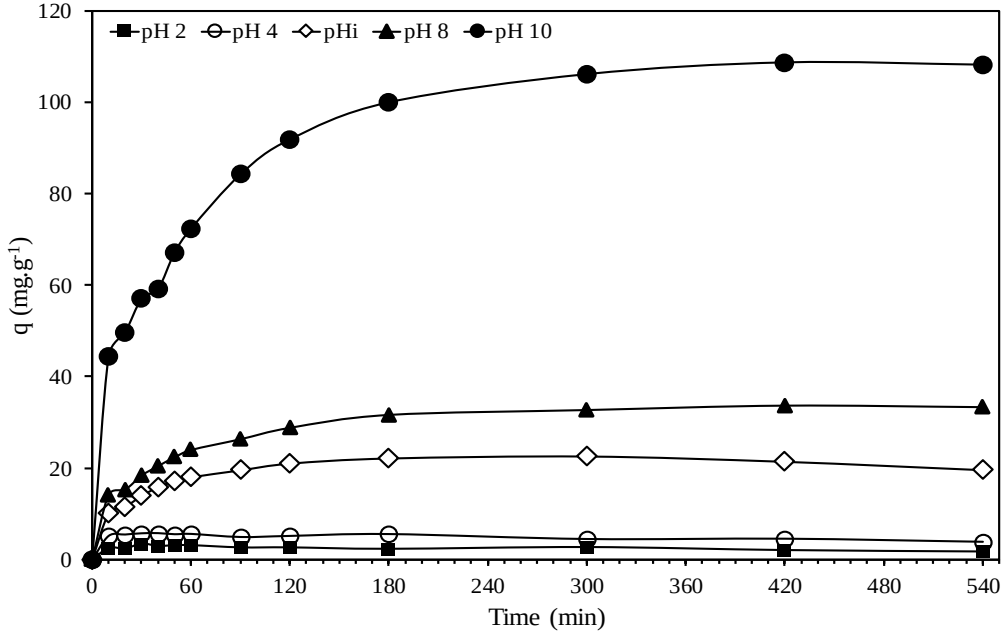
pH 2
pH 4
pHi
pH 8
pH 10
q (mg.g-1)
Time (min)
0
20
40
60
80
100
120
0
60
120
180
240
300
360
420
480
540

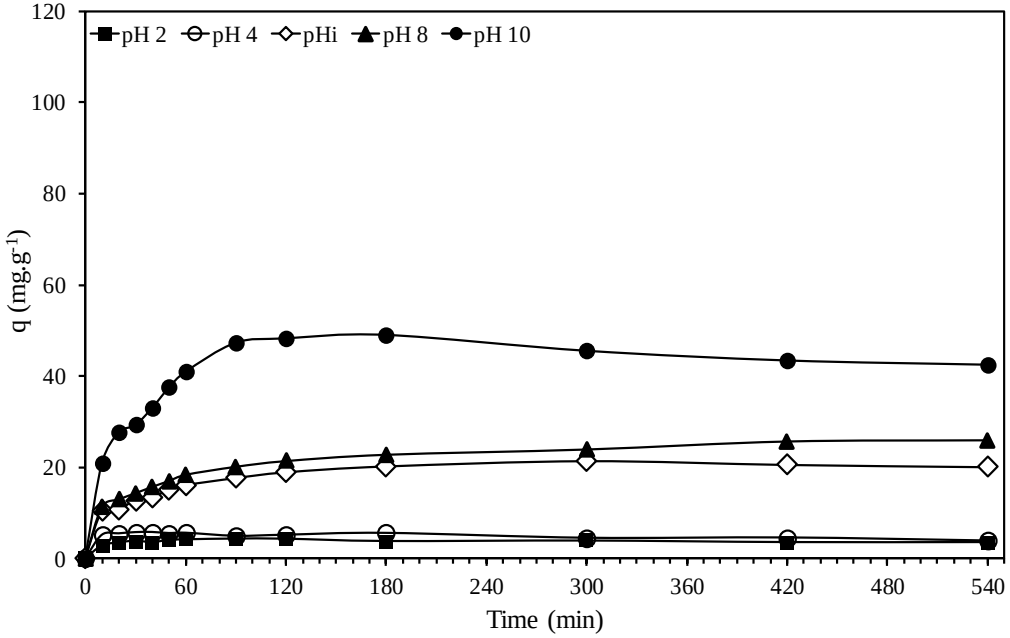
pH 2
pH 4
pHi
pH 8
pH 10
q (mg.g-1)
Time (min)
0
20
40
60
80
100
120
0
60
120
180
240
300
360
420
480
540

Figure 12

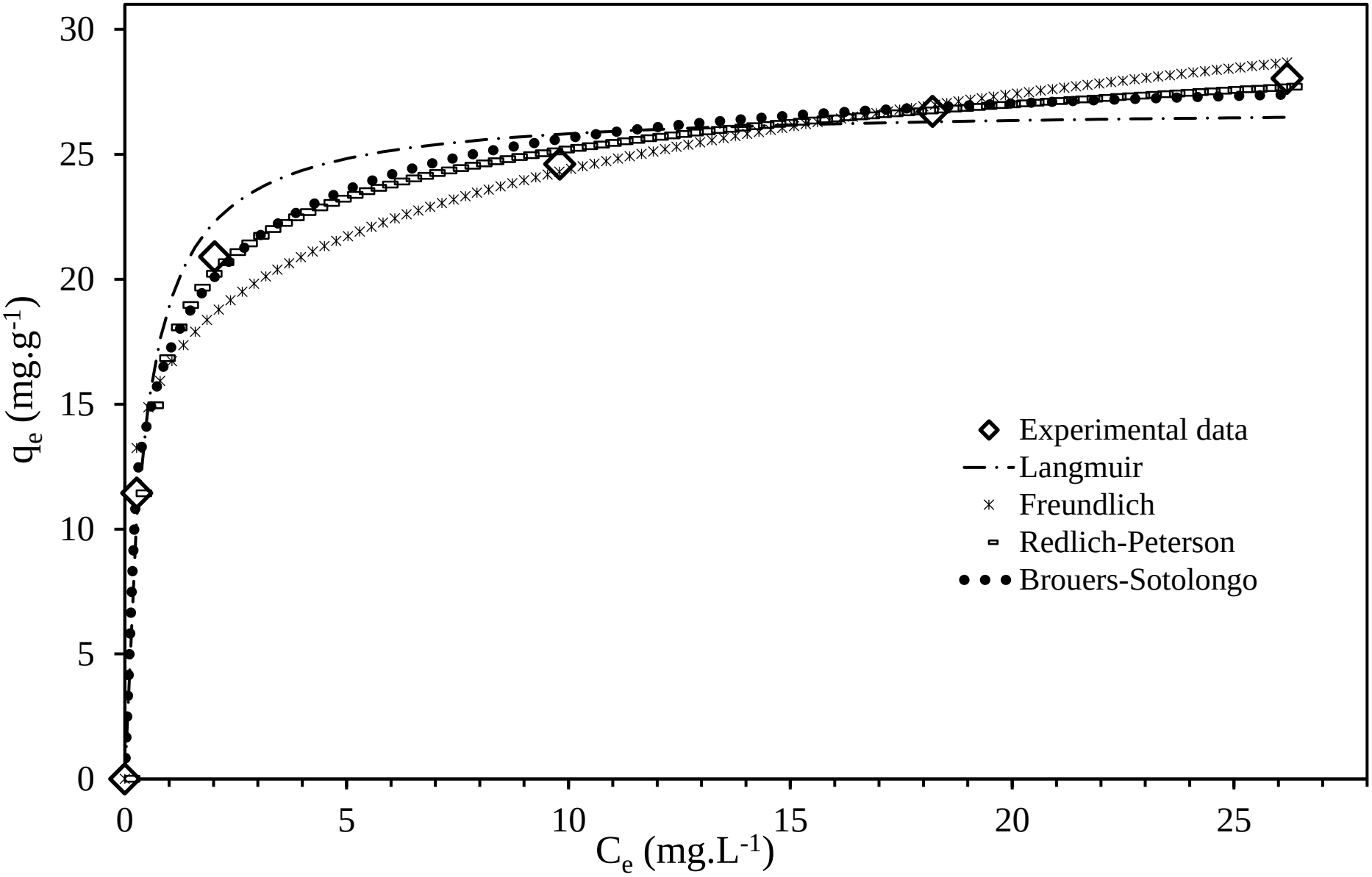
30
25
20
15
10
5
0
0
5
10
15
20
25
q_e (mg.g^{-1})
C_e (mg.L^{-1})
Experimental data
Langmuir
Freundlich
Redlich-Peterson
Brouers-Sotolongo

Supplementary Material

Click here to download Supplementary Material: Supplementary Figures_article.docx